Polynuclear Metal Hydrido Alkoxides. 2. Hydrogenation of 1,2-$W_2(^iBu)_2(O^iPr)_4$. Preparation, Characterization, and Some Reactions of $W_6H_5(C^iPr)(O^iPr)_{12}$, $W_2(H)_2(O^iPr)_4(dmpe)_2$, and $W_4(H)_4(dmpm)_3$, Where dmpe = Bis(dimethylphosphino)ethane and dmpm = Bis(dimethylphosphino)methane

Malcolm H. Chisholm,* Kirsten Folting, Keith S. Kramer, and William E. Streib

Contribution from the Department of Chemistry and Molecular Structure Center, Indiana University, Bloomington, Indiana 47405

Received December 19, 1996[⊗]

Abstract: H_2 and 1,2-$W_2(^iBu)_2(O^iPr)_4$ react in hydrocarbon solvents to give the cluster $W_6(H)_5(C^iPr)(O^iPr)_{12}$ (**1**) in 40% crystalline yield. $W_2(H)_2(O^iPr)_4(dmpe)_2$ (**2**) and $W_4(H)_4(O^iPr)_8(dmpm)_3$ (**3**) have been isolated in the presence of the chelating diphosphines $Me_2PCH_2CH_2PMe_2$ (dmpe) and $Me_2PCH_2PMe_2$ (dmpm). Reactions involving the use of various isotopes reveal the importance of both α- and β-CH activation of the ^{i}Bu ligand. An X-ray determination and NMR data reveal that **1** contains an octahedral W_6 unit, W−W = 2.58 to 2.85 Å, supported by four bridging hydride ligands, seven bridging alkoxides, and one bridging isobutylidyne ligand in addition to five terminal O^iPr and one terminal hydride: $W_6(H)(\mu\text{-}H)_4(\mu\text{-}C^iPr)(\mu\text{-}O^iPr)_7(O^iPr)_5$. Only one isomer is observed crystallographically, and the NMR data are indicative of its presence in solution. The cluster **1** is inert with respect to intramolecular ligand site exchange, which has allowed the detection of preferential hydrogenolysis and hydrogenation involving the terminal W−H ligand while alcoholysis occurs preferentially at the terminal W−O^iPr site adjacent to three μ-H ligands. In the solid state, compound **2** has four terminal O^iPr ligands on one W atom and two dmpe ligands on the other: $(^iPrO)_4W(\mu\text{-}H)_2W(dmpe)_2$, W−W = 2.49 Å. The locations of the two μ-H ligands are inferred from the X-ray determination and their proposed locations are consistent with the hydride-locating program XHYDEX. In solution, **2** is fluxional and low-temperature ^{1}H and $^{31}P\{^1H\}$ NMR spectra are consistent with the presence of two isomers, one of which is the same as that seen in the solid state while the other has the more symmetrical disposition of ligands $(dmpe)(^iPrO)_2W(\mu\text{-}H)_2W(O^iPr)_2(dmpe)$. Compound **3** contains a chain of four tungsten atoms with terminal W−W distances of ∼2.5 Å and a central W to W distance of 3.6 Å, bridged by three dmpm ligands. The solid-state molecular structure is proposed as $(^iPrO)_3W(\mu\text{-}H)(\mu\text{-}O^iPr)W(\mu\text{-}dmpm)_3(\mu\text{-}H)W(\mu\text{-}H)_2W(O^iPr)_4$. The solution NMR data reveal that **3** is fluxional but that at low temperatures a structure akin to that formulated above is present. These results are discussed in terms of the developing chemistry of hydrido alkoxides of the early transition elements.

Introduction

Since the initial discovery of $HCo(CO)_4$ and $H_2Fe(CO)_4$ in the 1930's,[1] the chemistry of metal hydrides and metal polyhydrides has been systematically developed with the support of ancillary ligands which are soft, π-acceptors such as tertiary phosphines, carbon monoxide, and the extended family of cyclopentadienyl and η^n-carbocyclic ligands.[2] As a result, the chemistry of the metal−hydride bond is intimately related to the development of organometallic chemistry and in particular plays a pivotal role in numerous stoichiometric and catalytic reactions.[2d] Subtle changes in the nature of such ancillary ligands may greatly change the reactivity of the M−H bond, which may range from basic (hydridic) to acidic (protic). It is, however, not necessary to have attendant soft ligands, and the formation of the $[Mo_2(H)Cl_8]^{3-}$ ion in the reaction between $Mo_2Cl_8^{4-}$ and *c*HCl(aq) provides a good example of a μ-hydrido ligand supported exclusively by hard donor ligands, chloride, formed in aqueous acid.[3]

As part of our interest in developing organometallic chemistry of the early transition elements supported by alkoxide ligands,[4] hydrido metal alkoxides of the general formula $M_xH_y(OR)_z$ are a particularly attractive group of complexes in terms of their potential reactivity.[5] Already it has been shown that niobium or tantalum hydrides supported by bulky aryloxide or trialkylsiloxide ligands can act as efficient all cis hydrogenation catalysts of arenes[6] and may reduce carbon monoxide in fascinating stepwise stoichiometric transformations.[7] Also $W_2(H)(OR)_7$ compounds have been shown to be selective in α-olefin hydrogenation.[8]

⊗ Abstract published in *Advance ACS Abstracts,* June 1, 1997.

(1) (a) Heiber, W. *Naturwissenschaften* **1931**, *19*, 360. (b) Heiber, W. *Adv. Organomet. Chem.* **1970**, *8*, 1.

(2) (a) Collman, J. P.; Hegedus, L. S.; Norton, J. R.; Finke, R. G. *Principles and Applications of Organotransition Metal Chemistry*; University Science Books: Mill Valley, CA, 1987. (b) Cotton, F. A.; Wilkinson, G. *Advanced Inorganic Chemistry*, 5th ed.; J. Wiley: New York, 1988. (c) Elschenbroich, C.; Salzer, A. *Organometallics*, 2nd ed.; VCH: Weinheim, 1992. (d) Parshall, G. W.; Steven, D. I. *Homogeneous Catalysis*, 2nd ed.; J. Wiley: New York, 1992.

(3) (a) Cotton, F. A.; Kalbacher, B. J. *Inorg. Chem.* **1976**, *15*, 522. (b) Bino, A.; Cotton, F. A. *Angew. Chem., Int. Ed. Engl.* **1979**, *18*, 332.

(4) (a) Chisholm, M. H. *Chemtracts: Inorg.* **1992**, *4*, 273. (b) Chisholm, M. H.; Rothwell, I. P. *Alkoxides and Related O-Donor Ligands in Organometallic Chemistry*; Polyhedron Symposium-in-Print, No. 16, 1995.

(5) Chisholm, M. H. *Chem. Soc. Rev.* **1995**, *24*, 79.

(6) (a) Yu, J. S.; Rothwell, I. P. *J. Chem. Soc., Chem. Commun.* **1992**, 623. (b) Yu, J. S.; Ankianiec, B. C.; Nguyen, M. T.; Rothwell, I. P. *J. Am. Chem. Soc.* **1992**, *114*, 1927. (c) Rothwell, I. P. *Chem. Soc. Feature* In press.

(7) (a) Toreki, R.; LaPointe, R. E.; Wolczanski, P. T. *J. Am. Chem. Soc.* **1987**, *109*, 7558. (b) Miller, R. L.; Toreki, R.; LaPointe, R. E.; Wolczanski, P. T.; Van Duyne, G. D.; Roe, D. C. *J. Am. Chem. Soc.* **1993**, *115*, 5570.

(8) Barry, J. T.; Chacon, S. T.; Chisholm, M. H.; Huffman, J. C.; Streib, W. E. *J. Am. Chem. Soc.* **1995**, *117*, 1974.

S0002-7863(96)04363-6 CCC: $14.00

Known routes to hydridometal alkoxides are currently rather limited and involve one of the following:[5] (1) reduction of a metal halide by Na/Hg in the presence of H_2; (2) oxidative addition of H_2 or ROH to a M−M multiple bond; (3) decomposition of a metal alkoxide; and (4) hydrogenolysis of metal−hydrocarbyl groups. In this paper we describe our studies of the reaction between $W_2(^iBu)_2(O^iPr)_4$ and H_2 in hydrocarbon solvents which lead to the most remarkable polynuclear hydrido metal alkoxide $W_6(H)_5(C^iPr)(O^iPr)_{12}$, originally mistaken to be $W_5(H)_5(O^iPr)_{13}$.[9] These studies include the use of a variety of isotopically labeled compounds and the introduction of chelating phosphines, $Me_2PCH_2CH_2PMe_2$ (dmpe) and $Me_2PCH_2PMe_2$ (dmpm), as traps for reactive intermediates. We also report on some of the reactions of the new compounds described herein. Preliminary reports of some aspects of this work have appeared.[10]

Results and Discussion

Synthesis. (a) $W_6(H)_5(C^iPr)(O^iPr)_{12}$ (1). The compound 1,2-$W_2(^iBu)_2(O^iPr)_4$ is thermally unstable in solution and reacts with PMe_3 according to eq 1.[11] By analogy with the known reaction involving 1,2-$Mo_2(CH_2Ph)_2(O^iPr)_4$ and PMe_3,[12] reaction 1i is believed to involve a PMe_3 promoted alkyl migration across

$$W_2(^iBu)_2(O^iPr)_4 + 3PMe_3 \xrightarrow[\text{hexane}]{22\ ^\circ C} (PMe_3)(^iPrO)_3W(\mu\text{-}H)(\mu\text{-}C^iPr)W(O^iPr)(PMe_3)_2 + {}^iBuH \quad (1i)$$

$$(PMe_3)(^iPrO)_3W(\mu\text{-}H)(\mu\text{-}C^iPr)W(O^iPr)(PMe_3)_2 \xrightarrow[\text{hexane}]{22\ ^\circ C} (PMe_3)(^iPrO)_2W(\mu\text{-}H)(\mu\text{-}C^iPr)W(O^iPr)_2(PMe_3) + PMe_3 \quad (1ii)$$

the M−M bond followed by α-CH activation leading to the elimination of ^{i}BuH and oxidative addition of the isobutylidene ligand to the ditungsten center giving the μ-hydrido, μ-isobutylidyne complex having the W_2^{10+} core. Reaction 1ii is a subsequent rearrangement to the symmetrical molecule involving a rate-determining dissociation of PMe_3. It was this kinetic lability of the 1,2-$W_2(^iBu)_2(O^iPr)_4$ compound, coupled with the presence of β-CH groups and the potential for H_2 oxidative addition across the W≡W bond,[13] that led us to examine its reactivity toward H_2. The reaction shown in eq 2 was thus discovered and the black, hydrocarbon-soluble, air-sensitive, crystalline cluster **1** was isolated in ca. 40% yield. By ^{1}H NMR spectroscopy compound **1** is the major species formed in reaction 2, but hydride signals other than those of **1** are also seen. Whether these are other isomers or other compounds is presently not known (see later). Compound **1** shows 5 hydride signals and 13 ^{i}Pr groups and it was the latter observation that first led to its formulation as $W_6(H)_5(O^iPr)_{13}$. However, when reaction 2 is carried out employing the labeled compound 1,2-$W_2(^iBu)_2(O^iPr\text{-}d_7)_4$, formation of $W_6(H)_5(C^iPr)(O^iPr\text{-}d_7)_{12}$ is clearly evident by ^{1}H NMR as one methine septet and two doublets arise from the C^{i}Pr group (the latter contains diastereotopic methyl groups as will be shown later).

$$1,2\text{-}W_2(^iBu)_2(O^iPr)_4 + H_2\ (3\ atm) \xrightarrow[\text{hexane}]{22\ ^\circ C} W_6(H)_5(C^iPr)(O^iPr)_{12} + {}^iBuH + Me_2C{=}CH_2 \quad (2)$$

We shall return to investigations pertinent to the mechanisms of the formation of **1** later. However, it was suspected early on in our studies that formation of the hexanuclear cluster occurred by way of the stepwise coupling of reactive W_2 fragments as for example in a hypothetical reaction, eq 3.[14] This led us to attempt a trapping of a reactive W_2 species by the addition of a chelating phosphine. Note a monodentate phosphine was known to promote α-CH activation, eq 1, while chelating phosphines could form adducts such as 1,2-$W_2(CH_2R)_2(O^iPr)_4$(dmpe).[11]

$$W_2(H)(C^iPr)(O^iPr)_4 + 2[W_2(H)_2(O^iPr)_4] \rightarrow W_6(H)_5(C^iPr)(O^iPr)_{12} \quad (3)$$
1

(b) $W_2(H)_2(O^iPr)_4(dmpe)_2$. When the reaction between 1,2-$W_2(^iBu)_2(O^iPr)_4$ and H_2 (3 atm) is carried out in the presence of dmpe, with the order of addition being H_2 after dmpe, then formation of **1** is impeded and the major product is $W_2(H)_2(O^iPr)_4$(dmpe)$_2$ (**2**), which is formed according to eq 4.

$$1,2\text{-}W_2(^iBu)_2(O^iPr)_4 + 2dmpe \xrightarrow[\text{hexane}]{H_2\ (3\ atm),\ 22\ ^\circ C} W_2(H)_2(O^iPr)_4(dmpe)_2 + {}^iBuH + Me_2C{=}CH_2 \quad (4)$$

Compound **2** is a dark-brown, hydrocarbon-soluble, air-sensitive, crystalline solid. When the reaction related to eq 4 is carried out with $Ph_2PCH_2CH_2PPh_2$ (dppe), the hexane-insoluble compound $W_2(H)_2(O^iPr)_4(dppe)_2$ is formed and precipitates from solution. The latter compound is soluble in toluene and benzene.

(c) $W_4(H)_4(O^iPr)_8(dmpm)_3$. The reaction between the methylene bridged diphosphine $Me_2PCH_2PMe_2$, dmpm, and 1,2-$W_2(^iBu)_2(O^iPr)_4$ in the presence of H_2 leads to the dark-brown, hydrocarbon-soluble, air-sensitive, crystalline compound $W_4(H)_4(O^iPr)_8(dmpm)_3$ (**3**), according to eq 5.

$$2W_2(^iBu)_2(O^iPr)_4 + 3dmpm \xrightarrow[22\ ^\circ C,\ \text{hexane}]{H_2\ (3\ atm)} W_4(H)_4(O^iPr)_8(dmpm)_3 + {}^iBuH + Me_2C{=}CH_2 \quad (5)$$

Solid-State and Molecular Structures of 1, 2, and 3. (a) $W_6(H)_5(C^iPr)(O^iPr)_{12}$ (1). A ball-and-stick stereoview of the hexanuclear cluster, **1**, is shown in Figure 1. This clearly reveals that the cluster is related to the well-known octahedral class of clusters having 12 bridging (μ_2) and 6 terminal ligands.[15] These

(9) Chisholm, M. H.; Kramer, K. S.; Streib, W. E. *J. Am. Chem. Soc.* **1992**, *114*, 3571; correction *J. Am. Chem. Soc.* **1995**, *117*, 6152.

(10) (a) Chisholm, M. H.; Kramer, K. S.; Lobkovsky, E. G.; Streib, W. E. *Angew. Chem., Int. Ed. Engl.* **1995**, *34*, 891. (b) Chisholm, M. H.; Kramer, K. S. *Chem. Commun.* **1996**, 1331.

(11) Blau, R. J.; Chisholm, M. H.; Eichhorn, B. W.; Huffman, J. C.; Kramer, K. S.; Lobkovsky, E. B.; Streib, W. E. *Organometallics* **1995**, *14*, 1855.

(12) Chisholm, M. H.; Folting, K.; Huffman, J. C.; Kramer, K. S.; Tatz, R. J. *Organometallics* **1992**, *11*, 4029.

(13) This has been seen previously in (i) the reversible addition of H_2 to $Cp'_2W_2Cl_4$ (Green, M. L. H.; Mountford, P. P. *Chem. Soc. Rev.* **1992**, *21*, 29) and (ii) in the reversible reaction between $W_2(X)_2$(silox)$_4$, where X = Cl and H, and H_2 (Miller, R. L.; Lawler, K. A.; Bennett, J. L.; Wolczanski, P. T. *Inorg. Chem.* **1996**, *35*, 3242).

(14) The coupling of $W_2(OR)_6$ compounds to give $W_4(OR)_4$ compounds has been well-documented. See, for example, where R = ^{i}Pr: Chisholm, M. H.; Clark, D. C.; Folting, K.; Huffman, J. C.; Hampden-Smith, M. J. *J. Am. Chem. Soc.* **1987**, *109*, 7750. Chisholm, M. H.; Clark, D. L.; Hampden-Smith, M. J. *J. Am. Chem. Soc.* **1989**, *111*, 574. And when R = $CH_2{}^c$Bu, $CH_2{}^c$Pen, $CH_2{}^i$Pr: Chisholm, M. H.; Folting, K.; Hammond, C. E.; Hampden-Smith, M. J.; Moodley, K. G. *J. Am. Chem. Soc.* **1989**, *11*, 5300.

(15) For $M_6(\mu\text{-}X)_{12}{}^{n+}L_6$ systems, where M = Sc, Y, Zr, Nb, Ta, Pr, Gd, Er, La, and Th and X = a halide, see: Cotton, F. A.; Hughbanks, T.; Runyan, C. E., Jr.; Wojtczak, W. A. In *Early Transition Metal Clusters with π-Donor Ligands*; Chisholm, M. H., Ed., VCH: Weinheim, 1995; Chapter 1 and references cited therein.

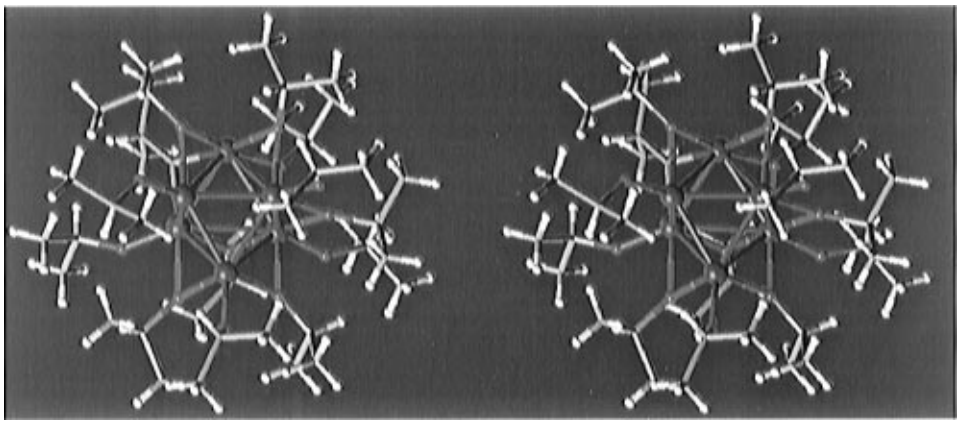

Figure 1. Stereoview of the $W_6(H)_5(C^iPr)(O^iPr)_{12}$ molecule as determined by single-crystal X-ray crystallography. The hydride ligands are not shown but are proposed to occupy the otherwise missing edge-bridging and terminal sites of an $M_6(\mu\text{-}X)_{12}X_6$ moiety. Tungsten atoms are green, oxygens are red.

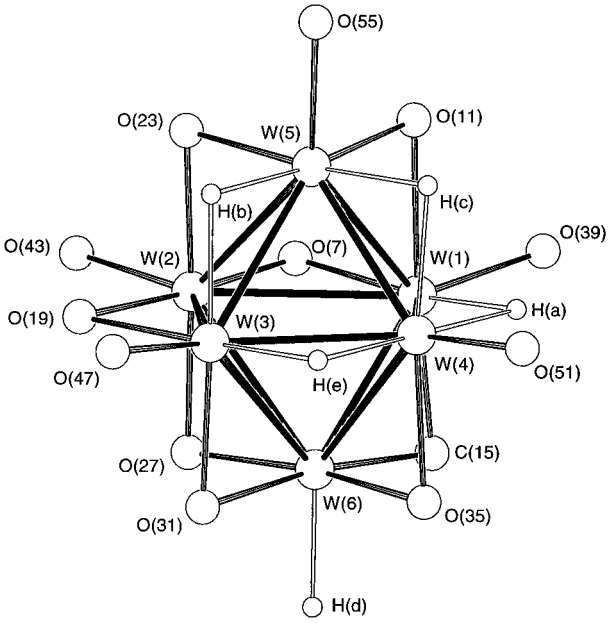

Figure 2. A ball-and-stick drawing of the $W_6(H)_5O_{12}C$ skeleton of the $W_6(H)_5(O^iPr)_{12}(C^iPr)$ molecule. The atom C(15) was refined as carbon, and the hydride ligands denoted are shown in the proposed locations and their labeling H(a)−H(e) is as described in the text.

are seen, for example, in lower valent zirconium, niobium, and tantalum halides and for the methoxide $Na_2Nb_6(\mu\text{-}OMe)_{12}(OMe)_6\cdot(MeOH)_x$.[16] What is evident, however, is that four edge bridges are apparently vacant as is one terminal site. It is in these positions that we propose there are hydride ligands, and the central $W_6H_5O_{12}C$ skeleton with the atom number scheme is given in Figure 2. Selected bond distances and bond angles are given in Tables 1 and 2, respectively. It is noteworthy that the μ-C^iPr ligand does not appear to be disordered with any of the other μ-O^iPr sites and *when C(15) was refined as carbon and not as oxygen the 10B_{iso} value dropped from 50 to 15*.

The terminal W−O distances span the range 1.95 to 2.02 Å while those of the bridging W−O groups are 2.02 to 2.21 Å, with the longest W−O distance being associated with a W−μ-OR bond that is trans to one of the W−μ-C bonds, namely W(1)−O(11). The other W−O bond trans to a W−C bond, W(6)−O(31) = 2.13 Å, is also relatively long, consistent with the view that the μ-isobutylidyne ligand exerts a higher trans influence than a μ-O^iPr ligand. In connection with the W−μ-O distances noted above, it is worth mentioning that W(1)−C(15) *appears* shorter, 1.97(2) Å, relative to W(6)−C(15), 2.02(2) Å, which would be consistent with the observation that W(1)−O(11) is longer than W(6)−O(31) based on the concepts of trans-influence.[17] However, within the criteria of 3σ these W−C distances are not deemed significantly different, but the W−C distances are notably shorter than the average W−μ-O distance

Table 1. Selected Bond Distances (Å) for $W_6(H)_5(C^iPr)(O^iPr)_{12}$ (**1**)

A−B	distance	A−B	distance
W(1)−W(2)	2.847(1)	W(3)−W(5)	2.665(1)
W(1)−W(4)	2.786(1)	W(3)−W(6)	2.808(1)
W(1)−W(5)	2.833(1)	W(3)−O(19)	2.087(9)
W(1)−W(6)	2.651(1)	W(3)−O(31)	2.06(1)
W(1)−O(7)	2.06(1)	W(3)−O(47)	1.970(1)
W(1)−O(11)	2.21(1)	W(4)−W(5)	2.582(1)
W(1)−O(39)	1.96(1)	W(4)−W(6)	2.773(1)
W(1)−C(15)	1.97(2)	W(4)−O(35)	2.08(1)
W(2)−W(3)	2.760(1)	W(4)−O(51)	1.98(1)
W(2)−W(5)	2.797(1)	W(5)−O(11)	2.02(1)
W(2)−W(6)	2.792(1)	W(5)−O(23)	2.08(1)
W(2)−O(7)	1.99(1)	W(5)−O(55)	1.95(1)
W(2)−O(19)	2.028(9)	W(6)−O(27)	2.02(1)
W(2)−O(23)	2.037(9)	W(6)−O(31)	2.13(1)
W(2)−O(27)	2.023(9)	W(6)−O(35)	2.06(1)
W(2)−O(43)	2.02(1)	W(6)−C(15)	2.02(2)
W(3)−W(4)	2.600(1)		

Table 2. Selected Bond Angles (deg) for $W_6(H)_5(C^iPr)(O^iPr)_{12}$ (**1**)

A−B−C	angle	A−B−C	angle
O(7)−W(1)−O(11)	84.5(4)	O(35)−W(4)−O(51)	90.4(4)
O(7)−W(1)−O(39)	101.8(4)	O(11)−W(5)−O(23)	88.7(4)
O(7)−W(1)−C(15)	98.4(5)	O(11)−W(5)−O(55)	91.5(4)
O(11)−W(1)−O(39)	81.9(4)	O(23)−W(5)−O(55)	94.8(4)
O(11)−W(1)−C(15)	175.5(5)	O(27)−W(6)−O(31)	86.0(4)
O(39)−W(1)−C(15)	94.1(6)	O(27)−W(6)−O(35)	169.0(4)
O(7)−W(2)−O(19)	76.4(4)	O(27)−W(6)−C(15)	99.1(5)
O(7)−W(2)−O(23)	90.0(4)	O(31)−W(6)−O(35)	83.4(4)
O(7)−W(2)−O(27)	92.8(4)	O(31)−W(6)−C(15)	172.4(5)
O(7)−W(2)−O(43)	86.9(4)	O(35)−W(6)−C(15)	91.2(5)
O(19)−W(2)−O(23)	87.3(4)	W(1)−O(7)−W(2)	89.5(4)
O(19)−W(2)− O(27)	89.9(4)	W(1)−O(11)−W(5)	84.0(4)
O(19)−W(2)−O(43)	90.5(4)	W(2)−O(19)−W(3)	84.8(3)
O(23)−W(2)−O(27)	176.9(4)	W(2)−O(23)−W(5)	85.6(4)
O(23)−W(2)−O(43)	85.1(4)	W(2)−O(27)−W(6)	87.3(4)
O(27)−W(2)−O(43)	93.7(4)	W(3)−O(31)−W(6)	84.2(4)
O(19)−W(3)−O(31)	89.8(4)	W(4)−O(35)−W(6)	84.1(4)
O(19)−W(3)−O(47)	89.5(4)	W(1)−C(15)−W(6)	82.6(6)
O(31)−W(3)−O(47)	94.0(4)		

(16) Chisholm, M. H.; Heppert, J. A.; Huffman, J. C. *Polyhedron* **1984**, *3*, 475.

(17) Appleton, T. G.; Clark, H. C.; Manzer, L. E. *Coord. Chem. Rev.* **1973**, *10*, 352.

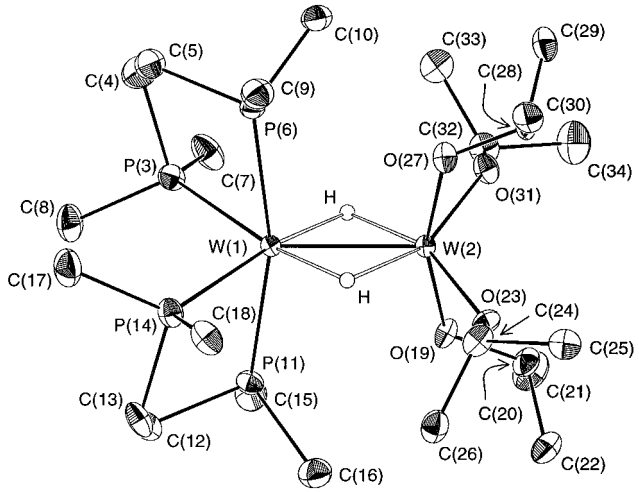

Figure 3. An ORTEP drawing of the $W_2(H)_2(O^iPr)_4(dmpe)_2$ molecule giving the atom number scheme used in the tables. The hydride ligands are shown as open circles in the proposed locations.

Table 3. Selected Bond Distances (Å) for $W_2(H)_2(O^iPr)_4(dmpe)_2$ (**2**)

A−B	distance	A−B	distance
W(1)−W(2)	2.4958(5)	W(2)−O(19)	1.982(5)
W(1)−P(3)	2.483(2)	W(2)−O(23)	1.935(5)
W(1)−P(6)	2.426(2)	W(2)−O(27)	1.982(5)
W(1)−P(11)	2.423(2)	W(2)−O(31)	1.940(5)
W(1)−P(14)	2.489(2)	P−C	1.84(1) av(5)
		O−C	1.41(1) av

by 0.1 Å as would be expected based on metric data for previously characterized compounds containing $W_2(\mu$-CR) and $W_2(\mu$-OR) groups.[18] There is no evidence of an HO^{i}Pr ligand based on W−OR distances since this would be expected to have a distance of ∼2.35 Å, which is well outside the observed range.[19]

Within the W_6 moiety the distances involving W(3)−W(5), W(3)−W(4), and W(4)−W(5) are notably shorter than the others, 2.61 Å (av), and of the others the shortest involves W(1)−W(6) = 2.65 Å, which is bridged by the μ-C^{i}Pr ligand. We have noted previously that $W_2(\mu$-CR) moieties tend to give short W−W distances due to a mixing of W d_π−W d_π and Cp_π orbitals.[18] The short W−W distances associated with the face involving W(3), W(4), and W(5) may similarly be understood if one accepts that each of these edges is proposed to be supported by bridging hydride ligands. Finally, it should be stated that while none of the proposed five hydride ligands was located crystallographically, the proposed locations as shown in Figure 2 are entirely satisfactory to the hydride locating program XHYDEX[20] and as will be shown later are supported by extensive NMR data.

(b) $W_2(H)_2(O^iPr)_4(dmpe)_2$ (2). An ORTEP drawing of the molecular structure of **2** is shown in Figure 3 where the proposed locations of the two μ-H ligands are denoted by circles. Again their presence in these positions is acceptable to the hydride locating program XHYDEX.[20] Selected bond distances and bond angles are presented in Tables 3 and 4.

The striking feature of the structure of **2** is that four O^{i}Pr ligands are bonded to W(2) while W(1) is bonded to four P atoms of two η^2-dmpe ligands. In this regard, the structure is similar to that of $Mo_2(O^iPr)_4(dmpe)_2$ but only superficially so.[21] In $Mo_2(O^iPr)_4(dmpe)_2$, the Mo−Mo distance is 2.236(1) Å, typical of a Mo−Mo triple bond distance for a compound having the M−M electronic configuration $\sigma^2\pi^4$, whereas in **2** the W−W distance is 2.496(1) Å, unmistakably outside the range for a related W≡W bond. Indeed, the distance falls squarely within the range of double bonds typically seen for $(W{=}W)^{8+}$-containing compounds having edge- or face-shared bioctahedral geometries.[22] In $Mo_2(O^iPr)_4(dmpe)_2$, all four Mo−Mo P angles fall within the range 98.0(1)° to 100.8(1)°,[21] whereas in **2** we see two sets of W−W−P angles, W(2)−W(1)−P(3),P(14) = 130.3°, W(2)−W(1)−P(6),P(11) = 97.5°. The W−P bonds with the more obtuse angles also are slightly longer, 2.48 *vs* 2.42 Å. A similar trend is seen for the W−O ligands with W−W−O = 99.3° (O(19) and O(27)) and 120.3° (O(23) and O(31)). Again the W−O distances fall into two sets, 1.98 and 1.94 Å, with the shorter bond distances correlating with the larger W−W−O angles. It should also be noticed that at W(1) the WP_4 fragment can be viewed as a ML_4 fragment derived from an octahedron where P(6)−W(1)−P(11) are remnants of a trans moiety. Similarly, at W(2) the O(19)−W(2)−O(27) moiety, with an angle of 161°, may be viewed as trans, and of the other O−W(2)−O angles four are less than 90° (85° (av)) and one, O(23)−W(2)−O(31), is 119°. Thus the geometry of **2** may be viewed as the co-joining of a pseudooctahedral (η^2-dmpe)$_2$W(H)$_2$ fragment to a W(O^{i}Pr)$_4$ fragment so as to form a highly distorted edge-shared bioctahedral dinuclear complex. The hydride ligands are formally trans to W(1)−P(3) and W(1)−P(14) bonds and W(2)−O(23) and W(2)−O(31) bonds.

Table 4. Selected Bond Angles (deg) for $W_2(H)_2(O^iPr)_4(dmpe)_2$ (**2**)

A−B−C	angle	A−B−C	angle
W(2)−W(1)−P(3)	130.20(5)	W(1)−W(2)−O(27)	99.0(2)
W(2)−W(1)−P(6)	97.13(5)	W(1)−W(2)−O(31)	120.1(2)
W(2)−W(1)−P(11)	97.85(5)	O(19)−W(2)−O(23)	84.6(2)
W(2)−W(1)−P(14)	130.43(5)	O(19)−W(2)−O(27)	161.3(2)
P(3)−W(1)−P(6)	78.39(7)	O(19)−W(2)−O(31)	86.5(2)
P(3)−W(1)−P(11)	91.51(7)	O(23)−W(2)−O(27)	86.4(2)
P(3)−W(1)−P(14)	99.37(7)	O(23)−W(2)−O(31)	119.4(2)
P(6)−W(1)−P(11)	165.01(7)	W(2)−O(19)−C(20)	123.8(5)
P(6)−W(1)−P(14)	91.93(7)	W(2)−O(23)−C(24)	131.9(5)
P(11)−W(1)−P(14)	78.68(7)	W(2)−O(27)−C(28)	123.9(4)
W(1)−W(2)−O(19)	99.7(2)	W(2)−O(31)−C(32)	134.9(5)
W(1)−W(2)−O(23)	120.5(2)		

(c) $W_4(H)_4(O^iPr)_8(dmpm)_3$ (3). A ball-and-stick drawing of the tetranuclear compound **3** is shown in Figure 4. The hydride ligands, which were not crystallographically located, are shown in locations by the open circles and are labeled H.

The structure has some resemblance to **2** in that there are two very different types of tungsten atoms. The terminal tungsten atoms are bonded to four O^{i}Pr ligands and to the internal tungsten atoms by W−W bonding, W(1)−W(2) = 2.451(1) Å and W(3)−W(4) = 2.498(1) Å. The central W atoms, W(2) and W(3), are not bonded but are bridged by three dmpm ligands and a proposed hydride (as shown in Figure 4). One alkoxide ligand bonded to W(1) forms a weak bridge to W(2) as evidenced by the asymmetry in the W−O distances: W(1)−O(26) = 2.03(1) Å *vs* W(2)−O(26) = 2.28(1) Å. In the proposed structure, with the location of the hydrides shown in Figure 4, all W atoms but W(1) are in a pseudooctahedral environment. W(1) has a coordination number of only 5 and may be viewed as a distorted trigonal bipyramid.

(18) Chisholm, M. H.; Folting, K.; Heppert, J. A.; Hoffman, D. M.; Huffman, J. C. *J. Am. Chem. Soc.* **1985**, *107*, 1234.
(19) See, for example, the structure of $Mo_4(OCH_2{}^cBu)_{12}(HOCH_2{}^cBu)$ in ref 14.
(20) Orpen, A. G. *J. Chem. Soc., Dalton Trans.* **1980**, 2509.
(21) Chisholm, M. H.; Huffman, J. C.; Van Der Sluys, W. G. *J. Am. Chem. Soc.* **1987**, *109*, 2514.
(22) Chisholm, M. H. *Polyhedron* **1983**, *2*, 681.

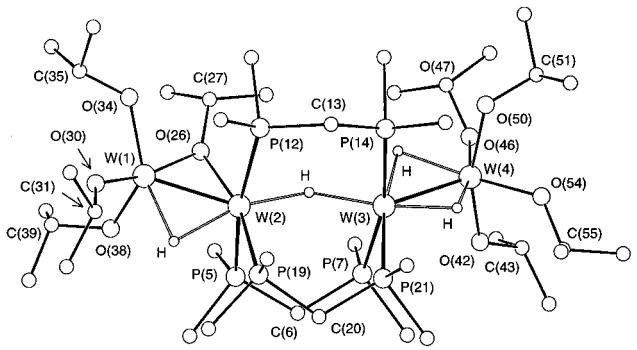

Figure 4. A ball-and-stick drawing of the $W_4(H)_4(O^iPr)_8(dmpm)_3$ molecule showing the atom number scheme used in the tables. The hydride ligands are shown as open circles and are placed in the proposed locations.

Table 5. Selected Bond Distances (Å) for $W_4(H)_4(O^iPr)_8(dmpm)_3$ (**3**)

A−B	distance	A−B	distance
W(1)−W(2)	2.451(1)	W(3)−W(4)	2.499(1)
W(1)−O(26)	2.03(1)	W(3)−P(7)	2.438(5)
W(1)−O(30)	1.93(1)	W(3)−P(14)	2.441(4)
W(1)−O(34)	1.89(1)	W(3)−P(21)	2.455(5)
W(1)−O(38)	1.90(1)	W(4)−O(42)	1.97(1)
W(2)−P(5)	2.449(5)	W(4)−O(46)	1.94(1)
W(2)−P(12)	2.472(5)	W(4)−O(50)	1.95(1)
W(2)−P(19)	2.442(4)	W(4)−O(54)	1.95(1)
W(2)−O(26)	2.28(1)	P−C	1.83(2) av
		O−C	1.44(2) av

The right-hand half of **3** can thus be seen to be related to **2** by the replacement of one W−P bond by a W−μ-H bond. Note two W(4)−W(3)−P angles are 93.7° while the other is larger, 122°. The $O_4W(4)$ fragment can also be viewed as being derived from an octahedron by the removal of a cis pair of ligands (these positions being, in fact, occupied by the two μ-H ligands). The trans O−W−O angle of 159.5° involves O(42) and O(50) and the W(4) to O(46) and O(54) bonds are trans to the μ-H−W(H) ligands. These are, as in **2**, slightly shorter W−O bonds than those that are mutually trans.

The unique coordination at W(1) arises because at least one tungsten atom has to be only five-coordinate, and with the hydride as shown in Figure 4, O(26) and O(38) occupy trans positions of a trigonal bipyramid while O(30) and O(34) are equatorial, *cf.* angles of 167° and 126°, respectively. The other O−W−O angles at W(1) are all close to 90°. Selected bond distances and angles are given in Tables 5 and 6, respectively.

NMR Solution Characterization of 1, 2, and 3. (a) $W_6(H)_5(C^iPr)(O^iPr)_{12}$ (1). The ^1H and $^{13}C\{^1H\}$ spectra of **1** in benzene-d_6 are entirely consistent with the expectations based on the solid-state structure shown in Figures 1 and 2. Of singular importance is the observation of five ^1H resonances, downfield of the benzene-d_6 aromatic protio impurity signal, at δ 14.65, 13.42, 13.40, 10.00, and 9.14, each flanked by satellites due to coupling to ^{183}W, $I = {}^1/_2$, 14.5% natural abundance, with $J_{^{183}W-^1H}$ ranging from 88 to 130 Hz. The integral intensity of the satellites of the resonance at 10.00 ppm is 15%, whereas the integral intensities of the others are *ca.* 22−25%, indicating that the former signal is assignable to a terminal hydride, $J_{^{183}W-^1H} = 130$ Hz, whereas the others are bridging two tungsten atoms. The assignment of the hydride ligands "a through e" as shown in Figure 2 is made possible by NOE difference spectroscopy and is supported by the observation that H(a) and H(e), being mutually trans, show a significant HH coupling, 10 Hz, and H(a) and H(c) show a small cis HH coupling, ∼1 Hz. The "missing terminal and edge-bridged sites" implicated in the stereoview of **1** (Figure 1) are indeed occupied by hydride ligands.

Table 6. Selected Bond Angles (deg) for $W_4(H)_4(O^iPr)_8(dmpm)_3$ (**3**)

A−B−C	angle	A−B−C	angle
W(2)−W(1)−O(26)	60.4(3)	P(7)−W(3)−P(14)	166.6(2)
W(2)−W(1)−O(30)	117.6(4)	P(7)−W(3)−P(21)	94.1(2)
W(2)−W(1)−O(34)	106.2(4)	P(14)−W(3)−P(21)	91.5(2)
W(2)−W(1)−O(38)	118.8(4)	W(3)−W(4)−O(42)	101.2(3)
O(26)−W(1)−O(30)	82.4(5)	W(3)−W(4)−O(46)	122.1(4)
O(26)−W(1)−O(34)	94.3(5)	W(3)−W(4)−O(50)	99.4(3)
O(26)−W(1)−O(38)	166.7(5)	W(3)−W(4)−O(54)	120.3(3)
O(30)−W(1)−O(34)	126.1(5)	O(42)−W(4)−O(46)	87.0(5)
O(30)−W(1)−O(38)	87.0(5)	O(42)−W(4)−O(50)	159.3(5)
O(34)−W(1)−O(38)	98.5(5)	O(42)−W(4)−O(54)	82.5(5)
W(1)−W(2)−P(5)	92.3(1)	O(46)−W(4)−O(50)	83.1(5)
W(1)−W(2)−P(12)	95.2(1)	O(46)−W(4)−O(54)	117.6(5)
W(1)−W(2)−P(19)	117.2(1)	O(50)−W(4)−O(54)	86.0(5)
W(1)−W(2)−O(26)	50.6(3)	W(1)−O(26)−W(2)	69.0(3)
P(5)−W(2)−P(12)	167.1(2)	W(1)−O(26)−C(27)	132(1)
P(5)−W(2)−P(19)	92.1(2)	W(2)−O(26)−C(27)	140(1)
P(5)−W(2)−O(26)	94.8(3)	W(1)−O(30)−C(31)	127(1)
P(12)−W(2)−P(19)	93.8(2)	W(1)−O(34)−C(35)	121(1)
P(12)−W(2)−O(26)	82.0(3)	W(1)−O(38)−C(39)	138(1)
P(19)−W(2)−O(26)	166.2(3)	W(4)−O(42)−C(43)	125(1)
W(4)−W(3)−P(7)	95.1(1)	W(4)−O(46)−C(47)	132(1)
W(4)−W(3)−P(14)	92.2(1)	W(4)−O(50)−C(51)	126(1)
W(4)−W(3)−P(21)	122.1(1)	W(4)−O(54)−C(55)	131(1)

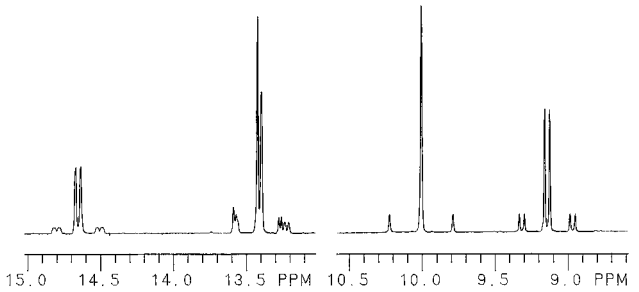

Figure 5. The five hydride signals associated with $W_6(H)_5(O^iPr)_{12}(C^iPr)$. The assignment of H(a) to H(e) as denoted in Figure 2 follows from H(a) being most downfield (to left) to H(e) most upfield (to right) in a consecutive order: a → b → c → d → e.

From the reaction of $W_2(^i Bu)_2(O^iPr\text{-}d_7)_4$ with D_2 in hydrocarbon solvents the labeled compound $W_6(D)_5(C^iPr)(O^iPr\text{-}d_7)_{12}$ is obtained, which shows a septet at δ 7.1 and two doublets δ 1.72 and 1.45 with $J_{HH} = 6$ Hz in the ^1H NMR spectrum assignable to the μ-C^iPr ligand. In the $^{13}C\{^1H\}$ NMR spectrum the $-C^iPr$ signal was found at δ 412.5, and by use of the labeled compound **1**-d_{89} the methyne carbon at δ 52.3 and the methyl carbon signals δ 35.7 and 32.2 were located for the isobutylidyne ligand. A careful inspection of the hydride region of the spectrum δ 15 to 9, Figure 5, shows trace protio impurities in each site H(a) through H(e) such that the reaction between D_2 and $W_2(^i Bu)_2(O^iPr\text{-}d_7)_{12}$ may have yielded not all **1**-d_{89} but at least some $W(H)(D_4)(\mu\text{-}C^iPr)(O^iPr\text{-}d_7)_{12}$ (**1**-d_{88}). Indeed, it is possible that the deuterated compound is **1**-d_{88} with a single hydride being, within the limits of experimental determination, statistically scrambled over the five hydride sites.

The 12 methine signals of the 12 chemically inequivalent O^iPr ligands of **1** appear as septets in the region δ 4.8 to 6.0 of the ^1H spectrum ($J_{HH} = 6$ Hz), and the methine carbons are seen as twelve signals δ 69.9 to 88.6 in the $^{13}C\{^1H\}$ NMR spectrum. The $CH(Me)_2$ doublets in the ^1H NMR spectra are not all distinct (several overlap), but in the $^{13}C\{^1H\}$ spectrum between 35.7 and 23.1 ppm there are 22 resonances, four of integral intensity twice that of the others—entirely consistent

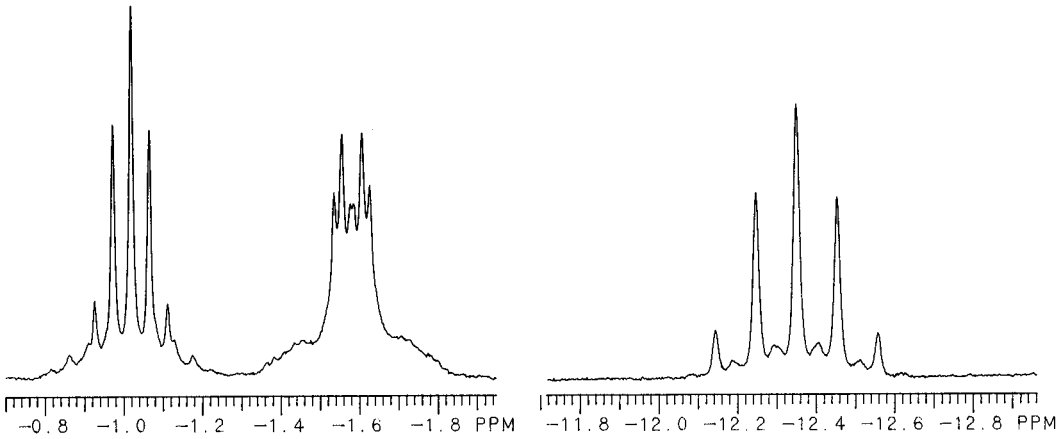

Figure 6. The hydride signals in the ^{1}H NMR spectrum of $W_2(H)_2(O^iPr)_4(dmpe)_2$ in toluene-d_8 at −60 °C, 500 MHz. The center resonance arises from isomer **A** and the outer resonances from isomer **B**.

with 13 diastereotopic O^{i}Pr-methyl groups. Full data are given in the Experimental Section.

In summary, the ^{1}H and ^{13}C NMR spectra are fully supportive of the existence of a *single isomer* of **1** in solution having the same structure as seen in the solid state.

(b) $W_2(H)_2(O^iPr)_4(dmpe)_2$ (2). The ^{1}H NMR specturm of **2** in toluene-d_8 at 22 °C shows only one type of O^{i}Pr ligand, no evidence of a hydride resonance (because it is in the baseline), and in the ^{31}P{^{1}H} NMR a single broad resonance centered at 14.9 ppm. The compound is evidently fluxional in solution as cooling to −60 °C in toluene-d_8 yields three hydride signals at δ −1.04, −1.60, and −12.4 in the integral ratio 3:4:3, respectively. These are shown in Figure 6. A ^{2}H NMR spectrum of the compound $W_2(D)_2(O^iPr)_4(dmpe)_2$, prepared from the reaction between $W_2(^i$Bu$)_2(O^iPr)_4$ and D_2 in the presence of dmpe, showed that these were the only ^{1}H resonances associated with hydride ligands. Relative to the methine proton signals the hydride resonances integrated in the ratio 1:2 consistent with the proposed formula $W_2(H)_2(O^iPr)_4$-$(dmpe)_2$.

The ^{31}P{^{1}H} spectrum of **2** in toluene-d_8 at 146 MHz gave upon cooling three resonances at δ 18.7, 14.4, and 5.91 in the integral ratio of 4:3:3, respectively. At 202 MHz the low-field signal (δ 18.7) was seen to be split into two resonances by 28 Hz due to the higher spectral resolution. Since proton-coupled ^{31}P NMR spectra showed only line broadening, a ^{31}P−^{31}P COSY spectrum was run at −60 °C to see if any ^{31}P−^{31}P coupling, unresolvable in the 1-D spectrum, could be detected. As shown in Figure 7, the upfield resonances which are resolved at 202 MHz and in the integral ratio 1:1 are indeed coupled as are the downfield signals. We thus propose that compound **2** exists in solution as a mixture of isomers shown in **A** and **B** below which interconvert rapidly on the NMR time scale at +60 °C.

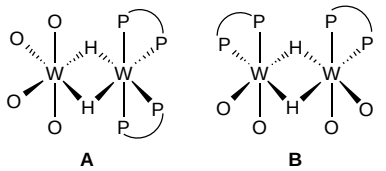

Isomer **A** is the same as that seen in the solid-state structure shown in Figure 3 while isomer **B** contains two chemically different hydrides which give rise to the ^{1}H NMR signals at δ −1.04 and −12.4.

(c) $W_2(H)_2(O^iPr)_4(dppe)_2$. $W_2(H)_2(O^iPr)_4(dppe)_2$, where dppe is $Ph_2PCH_2CH_2PPh_2$, is prepared similarly to compound **2** but employing dppe in place of dmpe. The compound has been characterized by elemental analysis and NMR spectroscopy, but a single crystal structure was not obtained. It is only sparingly soluble in benzene or toluene so NMR spectra were recorded in pyridine-d_5. The ^{31}P{^{1}H} spectrum gives rise to two sharp singlets flanked by satellites due to coupling to ^{183}W: δ 42, $J^{183}_{W-^{31}P} = 292$ Hz, and δ 25.8, $^1{}^{183}_{W-^{31}P} = 161$ Hz and $^2{}^{183}_{W-^{31}P} = 46$ Hz. In the ^{1}H NMR spectrum there is a single hydride resonance at δ 0.01 which integrates in the ratio 1:2 with the OC*H*Me$_2$ protons and appears as a multiplet of the type shown in Figure 6 (δ 1.60). The spectral data are consistent with a structure for $W_2(H)_2(O^iPr)_4(dppe)_2$ akin to that observed for **2** in the solid state and shown in Figure 3.

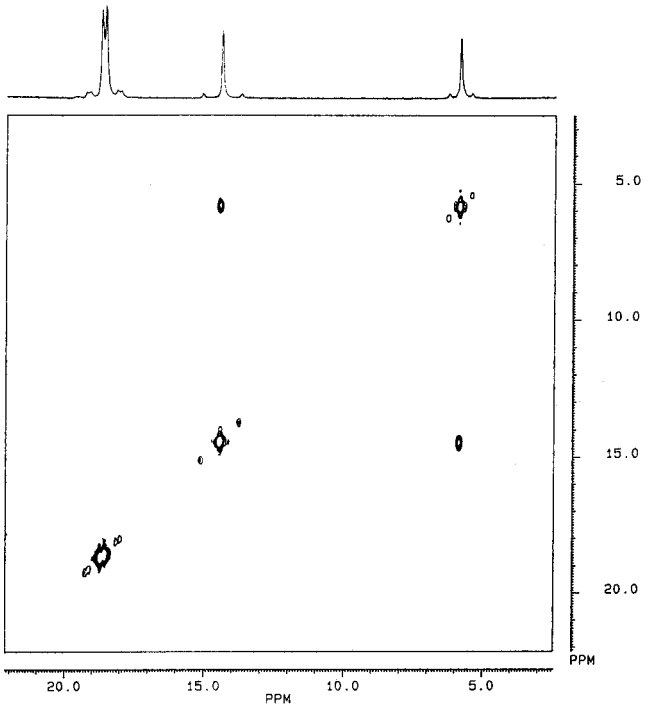

Figure 7. ^{31}P−^{31}P COSY of $W_2(H)_2(O^iPr)_4(dmpe)_2$ in toluene-d_8 at −60 °C. The 1D spectrum shown on top gives rise to four resonances. The two upfield resonances are due to isomer **A** and the two downfield to isomer **B** as defined in the text.

(d) $W_4(H)_4(O^iPr)_8(dmpm)_3$ (3). Although the ligand dmpm is well known to bridge M−M bonded metal centers,[23] as indeed it does in the solid-state structure of 1,2-$W_2(^i$Bu$)_2(O^iPr)_4$-$(dmpm)$,[11] the solution NMR data obtained for **3** in toluene-d_8

(23) Cotton, F. A.; Walton, R. A. In *Multiple Bonds Between Metal Atoms*, 2nd ed.; Oxford University Press: New York, 1993.

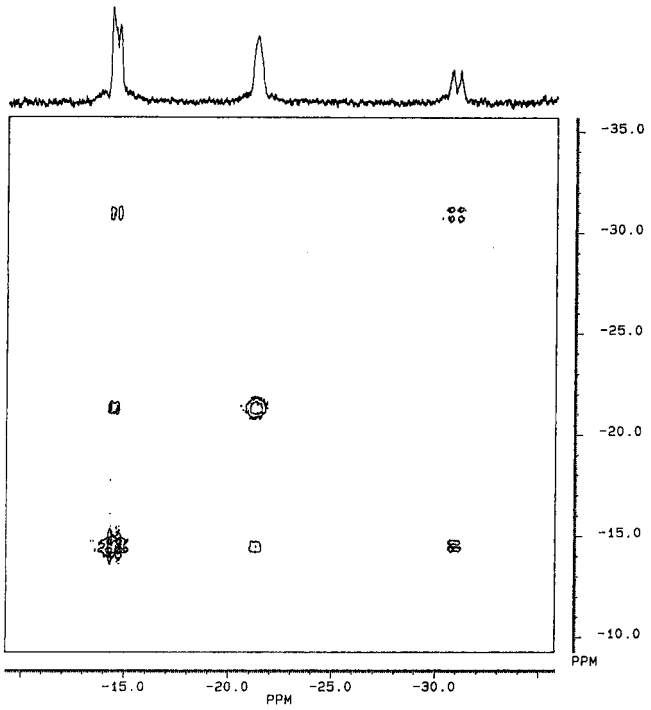

Figure 8. $^{31}P-^{31}P$ COSY of $W_4(H)_4(O^iPr)_8(dmpm)_3$ in toluene-d_8 at −60 °C.

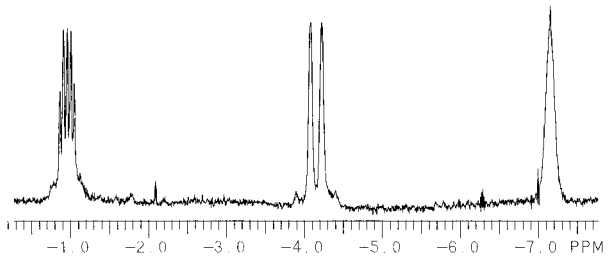

Figure 9. ^1H NMR spectrum recorded in toluene-d_8 at −60 °C, 500 MHz, showing three of the hydride resonances attributed to $W_4(H)_4(O^iPr)_8(dmpm)_3$.

indicate that the tetranuclear structure is maintained in solution, even at high temperatures (+80 °C), where the ^1H NMR spectrum shows three types of P*Me*$_2$ resonances in the integral ratio 4:4:4. We believe that this represents a time-averaged spectrum where a fluxional process makes equivalent the left and right halves of the W_4 chain such that a pseudomirror plane contains one dmpm ligand [P(19) and P(21) in Figure 4] and the four W atoms. Unfortunately the $^{31}P\{^1H\}$ spectrum is of little assistance because of poor line shape, unresolved coupling, and coincidental overlap. However, at −60 °C we find support for the maintenance of the solid-state structure. There are three complex multiplets in the $^{31}P\{^1H\}$ spectrum which integrate in a 1:2:3 ratio consistent with an AM_2XX_2' spectrum. A $^{31}P-^{31}P$ COSY spectrum, see Figure 8, recorded at −60 °C indicated that the resonance at δ −15.1 ppm was coupled to both of the other signals which were not coupled to each other. Assuming that neither through-ring (chain) nor cis P−P coupling is observed, the coupling information is consistent with the formulation that the left- and right-hand sides of the molecule are not under rapid exchange. It is also noteworthy that three of the expected four hydride signals were readily observed at −60 °C in the integral ratio 1:1:1 as shown in Figure 9. Of these resonances one is a doublet with a large $^{31}P-^1H$ coupling consistent with its placement trans to a single W−P bond (see Figure 4). Another resonance appears as a doublet of triplets wherein the outer lines overlap to give an apparent 1:2:2:2:1 pentet ($^2J_{^{31}P-^1H}$ = 30, 15 Hz). The third resonance is an ill-resolved multiplet while the fourth hydride signal is assumed to be obscured by the ^1H signals of the dmpm or OCHM*e*$_2$ protons. Collectively these data suggest that only one isomer is present in solution and that the tetranuclear nature of the complex is maintained.

Mechanistic Studies Aimed at Elucidating the Reaction Pathway Leading to the Formation of 1. It is reasonable to suggest that compound **1** arises from the formal coupling of three reactive dinuclear fragments as shown in eq 6. We have

$$2[W_2(H)_2(O^iPr)_4] + [W_2(H)(C^iPr)(O^iPr)_4] \rightarrow W_6(H)_5(C^iPr)(O^iPr)_{12} \quad (6)$$
1

seen how the addition of monodentate phosphines and nitrogen Lewis bases to 1,2-$W_2(CH_2R)_2(O^iPr)_4$ compounds can promote α-CH activation and the formation of compounds of the type $W_2(H)(CR)(O^iPr)_4L_2$, e.g. for R = ^{i}Pr and L = PMe_3 as shown in eq 1.[11] Furthermore, in the reaction of 1,2-$W_2(CH_2R)_2(O^i$-$Pr)_4$ compounds, where R = Et, with internal alkynes it was noted that for R = Et competing α- and *β*-CH activation pathways were possible with the latter leading to $W_2(\mu$-$C_2R'_2)_2(O^iPr)_4$ compounds (R′ = Me, Et) and the elimination of $CH_3CH_2CH_3$ and $MeCH{=}CH_2$.[24]

In order to investigate some of the reactions occurring when hydrocarbon solutions of $W_2(^i$Bu$)_2(O^iPr)_4$ are exposed to H_2, the volatile components were analyzed by GC-MS and NMR spectroscopy. Similar reactions and analyses were performed employing D_2 gas, and the reactions were also carried out in the presence of ethylene and dmpe. The results are summarized in Scheme 1, where the percentages of the various products are believed to be accurate to ±5% but the absolute ratios are not deemed significant with respect to a partitioning of the various pathways since the concentrations of the various species present in solution [W_2], [H_2], or [D_2] and [ethylene] are not known.

In the reaction between 1,2-$W_2(^i$Bu$)_2(O^iPr)_4$ and H_2 the formation of isobutylene, $Me_2C{=}CH_2$, clearly implicates a *β*-CH activation pathway where the uptake of H_2 at the dinuclear center promotes "alkyl group disproportionation": "$M_2(^i$Bu$)_2$" → "M_2" + ^{i}BuH + $Me_2C{=}CH_2$. The *ca.* 90% formation of isobutane could result from this reaction followed by hydrogenation of the isobutylene by a reactive species such as "$W_2(H)_2(O^iPr)_4$" as well as by α-CH activation, with the latter leading to "$W_2(H)(C^iPr)(O^iPr)_4$".

Further evidence for the importance of **both** α- and *β*-CH activation pathways is seen in the reactions with D_2 gas and D_2 and C_2H_4. In the case of the former, some 22% all protio ^{i}BuH was observed. This must represent the sum of ^{i}BuH formed by both α-CH and *β*-CH elimination pathways. [Note in these experiments we do not observe any D incorporation into the O^iPr ligands nor do we observe by NMR spectroscopy any C−H activation of the solvent. The ^{i}BuH once formed is inert with respect to incorporation of D by the introduction of D_2 gas in the presence of tungsten species present in solution.] Also the *ca.* 23% formation of $(CH_3)_2(CH_2D)CD$ clearly suggests that a reactive tungsten species is capable of hydrogenating isobutylene—though not very efficiently as some isobutylene is present in the gaseous mixture (<10%). The *ca.* 50% formation of the single deuterated product $(CH_3)_2(CH_2D)CH$ implicates a direct hydrogenolysis of the alkyl ligands. However, this could proceed via a *σ*-bond metathesis mechanism,

(24) Chisholm, M. H.; Eichhorn, B. W.; Huffman, J. C. *Organometallics* **1987**, *6*, 2264.

Scheme 1

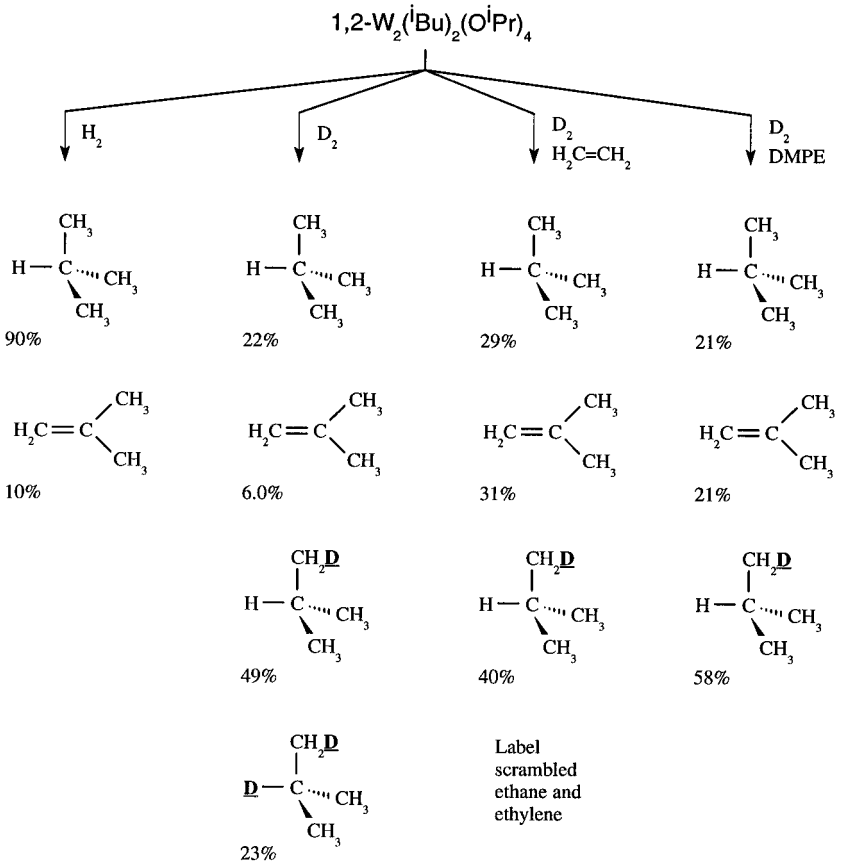

eq 7, or by an oxidative-addition/reductive-elimination sequence, eq 8.

$$1,2\text{-}W_2(CH_2{}^iPr)_2(O^iPr)_4 + D_2 \rightarrow 1,2\text{-}W(D)(CH_2{}^iPr)(O^iPr)_4 + (CH_2D)CH(CH_3)_2 \quad (7i)$$

$$1,2\text{-}W_2(D)(CH_2{}^iPr)(O^iPr)_4 + D_2 \rightarrow W_2(D)_2(O^iPr)_4 + (CH_2D)CH(CH_3)_2 \quad (7ii)$$

$$1,2\text{-}W_2(CH_2{}^iPr)_2(O^iPr)_4 + D_2 \rightarrow W_2(D)_2(CH_2{}^iPr)_2(O^iPr)_4 \quad (8i)$$

$$W_2(D)_2(CH_2{}^iPr)_2(O^iPr)_4 \rightarrow W_2(D)(CH_2{}^iPr)(O^iPr)_4 + (CH_2D)CH(CH_3)_2 \quad (8ii)$$

Reactive species such as $W_2(D)(CH_2{}^iPr)(O^iPr)_4$ could also enter into reductive elimination to give "$W_2(O^iPr)_4$" and $(CH_2D)CH(CH_3)_2$ or α-CH activation to give "$W_2(H)(C^iPr)(O^iPr)_4$". While we cannot distinguish between these pathways, we do emphasize that formation of $(CH_2D)CH(CH_3)_2$ implicates a hydrogenolysis by either (7) or (8).

In the presence of ethylene (excess) the reaction between 1,2-$W_2(^iBu)_2(O^iPr)_4$ and D_2 yields all protio isobutane and all protio isobutylene in essentially the same ratio. This suggests that in the presence of ethylene the isobutane is formed by the β-CH activation pathway, and the lack of D_2 incorporation to give $(CH_2D)CD(CH_3)_2$ indicates that $Me_2C{=}CH_2$ is not competitive with ethylene in hydrogenation. The formation of $(CH_2D)CH(CH_3)_2$ indicates that a hydrogenolysis pathway, either (7) or (8), is still operative while the formation of D-labeled ethane and ethene implicates reactive species such as $W_2(H)_2(O^iPr)_4$ that are capable of **both** reversible insertion with ethylene and hydrogenolysis of a W−Et moiety.

Again in the reaction between 1,2-$W_2(^iBu)_2(O^iPr)_4$ and D_2 in the presence of dmpe all protio isobutane and isobutylene are formed in equal quantities implicating the β-CH activation pathway. The formation of $(CH_2D)CH(CH_3)_2$ implicates hydrogenolysis. In this reaction, $W_2(D)_2(O^iPr)_4(dmpe)_2$ rather than compound **1** is the product.

In summary, while the formation of the isobutylidyne ligand must occur by α-CH activation, there is overwhelming evidence that β-CH activation is also extremely important in the formation of **1**. Indeed, in reactions between other 1,2-$W_2(R)_2(O^iPr)_4$ compounds where R lacks a β-hydrogen, related clusters are not formed. Reactive species "$W_2(H)_2(O^iPr)_4$" are implicated by the trapping reactions involving dmpe and dmpm which give **2** and **3**, respectively. It may well be that such species in the absence of bidentate ligands associate to give "$W_4(H)_4(O^iPr)_4$", which in turn reacts with 1,2-$W_2(^iBu)_2(O^iPr)_4$ to yield **1** with the elimination of ^{i}BuH. The order of these events is of course uncertain, but it should be recalled that the reaction between 1,2-$W_2(^iBu)_2(O^iPr\text{-}d_7)_4$ and D_2 leads to a cluster where some protio W−H bonds can be detected at each of the sites "a" through "e" in Figure 2. It seems then that this residual protio impurity in **1**-d_{89} must arise from the α-CH of an ^{i}Bu ligand. That it is distributed over the five W−H sites, at least to a detectable extent, suggests there is a degree of dynamic freedom in the assembly of the cluster compound **1** that is not subsequently available to the cluster **1** itself, *vide infra*.

Reactions of 1. The hydride ligands in **1** do not show any exchange in toluene-d_8 in the presence of 100 equiv of ^{i}PrOD from which we conclude that they are neither acidic nor basic. The reaction between **1** and $(CD_3)_2CDOD$, 100 equiv, in benzene-d_6 or toluene-d_8 showed a slow but selective alcoholysis

reaction ($t_{1/2}$ ~10 h, 33 °C) to yield $W_6(H)_5(C^iPr)(O^iPr)_{11}(O^i$-Pr-$d_7$) (**1**-$d_7$). Clearly one site in **1** is kinetically more labile toward alcoholysis than the others by roughly one order of magnitude. The question that arises is which one?

Having assigned the hydride resonances H(a) through H(e) as shown in Figure 2 by NOE difference spectroscopy, the influence of NOE between the hydride ligands and the methyne proton resonances was investigated. In this way several of the methine resonances could be assigned. For example, the methine resonance at δ 4.98 is assignable to the terminal alkoxide bound to W(5) because it is enhanced when both H(b) and H(c) are irradiated. Likewise the resonance at δ 4.84 is assigned to the alkoxide bound terminally to W(3) because it shows NOE to hydrides H(b) and H(e). The methine signal at δ 5.10, corresponding to the labile alkoxide, was enhanced by irradiation at H(c) (but not by irradiation of H(a) or H(e)). Thus the labile alkoxide must be either the one bridging W(1) and W(5) or the one bound terminally to W(4). At this point it should be remembered that the NOE between the OC*H*Me_2 protons and the hydride signals is determined by H- - -H distances and the latter are a consequence of preferred conformations.

In an attempt to make an unequivocal assignment the cluster **1** was allowed to react in benzene-d_6 with MeOH (10 equiv). This led to the disappearance of the methine signal at δ 5.10 and the growth of a singlet at δ 4.76 due to the formation of methoxide. As the new singlet at δ 4.76 grew in so did five new resonances a′ through e′ in the hydride region consistent with the formation of the cluster compound $W_6(H)_5(C^iPr)(O^i$-Pr)$_{11}$(OMe). The new hydride signals were closely related to their parent signals in that H(a′) and H(e′) were coupled, J_{HH} ~11 Hz, H(d′) had the largest value of $J^{183}{}_{W-^1H}$, and its satellite intensity was indicative of coupling to one tungsten, etc. Irradiation of the OMe signal at δ 4.76 showed NOE to H(a′), H(c′), and H(e′), thereby indicating that the kinetically labile site is the terminal OR group on W(4), denoted by O(51) in Figure 2, which is adjacent to three hydride ligands. In retrospect this makes good chemical sense since the terminal W−OR group involving W(4) is the least sterically congested, and we expect that terminal OR groups would be more labile to alcoholysis than bridging ones. It is, however, an extremely rare situation that bridge terminal site exchange is so slow that this can be observed.[25]

In order to probe further the reactivity of cluster **1**, the labeled compounds $W_6(D)_5(C^iPr)(O^iPr)_{12}$ (**1**-d_5) and $W_6(D)_5(C^iPr)(O^i$-Pr-$d_7)_{12}$ (**1**-d_{89}) were prepared. Compound **1**-d_5 was heated in benzene-d_6 at 33 °C for 4 weeks and the ^{1}H NMR spectrum recorded. No W−D for C−H scrambling was observed. Thus there is no evidence for reversible β-H elimination from O^{i}Pr ligands—at least none that leads to scrambling with the hydrides of the cluster **1**. The compound **1**-d_{89} was dissolved in benzene-d_6 and allowed to react with H_2 (3 atm) in a J. Young NMR tube. In this reaction slow, but site-selective exchange of H for D was seen at the terminal hydride H(d) with $t_{1/2}$ ~ 2 days at 33 °C. A slower but also site-selective H for D exchange was observed for one of the bridging hydrides, namely H(a). The relative rates of H for D exchange for H(d) to H(a) was *ca*. 4:1. After removal of H_2 gas the partially protio cluster containing H at sites H(d) and H(a) remained unaltered for 4 weeks at 33 °C. Thus, no scrambling of hydride ligands occurs within the cluster on a chemically significant time scale.

(25) In $Re_3(\mu$-O^{i}Pr)$_3$(O^{i}Pr)$_6$ the terminal sites show selective O^{i}Pr exchange in the presence of both acetone-d_6 and ^{i}Pr-d_7-OH because of the reversible reaction: $Re_3(\mu$-O^{i}Pr)$_3$(O^{i}Pr)$_6$ ⇌ $Re_3(\mu$-O^{i}Pr)$_3$(O^{i}Pr)$_5$(H) + acetone. The O^{i}Pr ligand bonded to the Re−H moiety is then capable of undergoing alcoholysis: Hoffman, D. M.; Lappas, D.; Wierda, D. A. *J. Am. Chem. Soc.* **1989**, *111*, 1531; **1993**, *115*, 10538.

Scheme 2

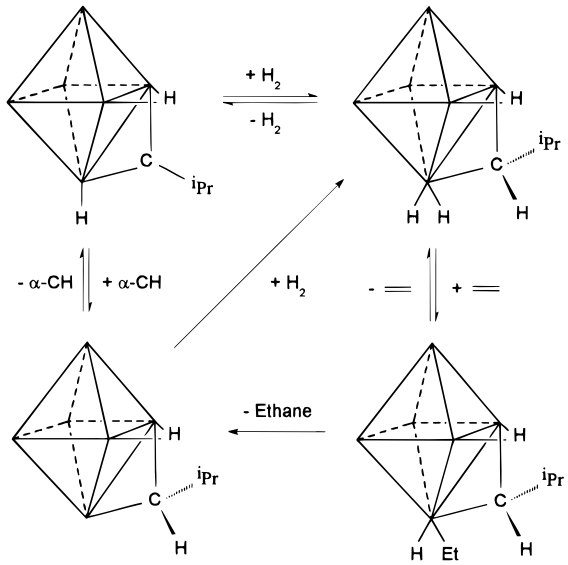

The cluster **1** dissolved in benzene-d_6 was allowed to react with 10 equiv of ethylene and H_2 (3 atm) in J. Young NMR tubes. The reaction was followed by ^{1}H NMR spectroscopy. Ethane was produced very slowly, *ca.* 2 equiv per week. An analogous reaction was undertaken employing **1**-d_{89}, ethylene, and H_2 (3 atm). Again ethane was produced and H was slowly incorporated into **1**-d_{89} at sites H(d) and H(a). Some deuterium was also detected in the ethane and ethylene. The rate of ethane formation was comparable but slightly slower than the H for D exchange of the hydrides at sites H(d) and H(a). The incorporation of D into ethylene and ethane in the above implicates the cluster in catalysis and led us to investigate the reaction between **1**-d_{89} and ethylene, C_2H_4. In this instance very little H for D exchange was observed, which leads us to suspect that insertion of ethylene into the terminal W−H(d) ligand may not be responsible for the formation of ethane.

An alternative pathway by which both hydride H for D exchange and ethylene hydrogenation could occur is shown in Scheme 2. Migration of an adjacent hydride to the μ-alkylidyne to generate an alkylidene ligand, which is in itself the microscopic reverse of the reaction leading to the formation of the μ-isobutylidyne ligand, would be equivalent to an intramolecular redox reaction of the cluster and would open up a vacant coordination site. As shown in Scheme 2, this could then lead to oxidative addition of H_2 and by reaction with ethylene lead to ethane. A direct addition of H_2 across the M−C multiple bond is also possible. These possibilities are attractive to us in light of the fact that H/D site exchange at the cluster occurs at roughly the same rate as ethylene hydrogenation and only sites H(d) and H(a) are involved. These hydrides are both adjacent to the alkylidyne ligand.

The reactivity of **1** toward $(CD_3)_2C{=}O$ and $(CH_3)_2{}^{13}C{=}O$ in benzene-d_6 was also investigated, and it was found that deuterated, $OCH(CD_3)_2$, or ^{13}C-labeled alkoxide ligands were incorporated selectively at the terminal W(4)−OR site. In these experiments protio acetone and ^{13}C-acetone were formed, respectively. Careful studies of these reactions revealed that the rate of incorporation of label into the cluster was dependent upon the presence of adventitious ^{i}PrOH, present as an impurity due to trace hydrolysis of the cluster. Furthermore, the exchange reaction shown in eq 9 occurred significantly faster, as deduced from NMR studies, than did incorporation of label into the cluster. From this observation we conclude the cluster is itself not directly responsible for the catalysis of the MPV reaction

$$(CH_3)_2{}^{13}C{=}O + (CD_3)_2CDOD \rightleftharpoons (CH_3)_2{}^{13}CDOD + (CD_3)_2C{=}O \quad (9)$$

9,[26] but rather catalysis arises from some species present in trace amounts due to degradation of the cluster. However, the site-selective alcoholysis involving W(4) allows incorporation of the label into the cluster.

A Minor Isomer of 1 and Related Cyclopentoxides and Cyclohexoxides? As noted earlier, compound **1** is prepared from the reaction between 1,2-$W_2(^i Bu)_2(O^i Pr)_4$ and H_2 in hydrocarbon solvents, eq 2, and is isolated in *ca*. 40% crystalline yield. Related compounds are believed to be formed in the reactions of 1,2-$W_2(^i Bu)_2(OR)_4$ and H_2, where R = ^{c}hexyl and ^{c}pentyl, based on the observation of hydride resonances similar to those characteristic for hydride signals observed for **1**. However, in the crude reaction mixture there are other signals in the hydride region. One compound that can be identified by its hydride signals is possibly an isomer of **1** because its hydride resonances integrate as 2:2:1, *i.e.* it contains 5 H. In the case of the reactions involving OR = O^{c}hexyl and O^{c}pentyl, these signals are present in a larger relative abundance than for R = ^{i}Pr. While we have not been able to isolate these compounds in a pure form, for R = ^{i}Pr it is possible to account for the compound as an isomer of **1**. The data δ 12.2, $J^{183}{}_{W-^1H} = 101$ Hz, $I = 24\%$ (1H), δ 11.8, $J^{183}{}_{W-^1H} = 108$ Hz, $I = 24\%$ (2H), and δ 8.3, $J^{183}{}_{W-^1H} = 132$ Hz, $I = 14\%$ (2H), implicate three bridging hydrides, two of which are equivalent, and two equivalent terminal hydrides. Thus an isomer of **1** having a mirror plane of symmetry would meet these requirements, and by merely exchanging the bridging hydride H(a) with the terminal alkoxide O(39) in Figure 2 such an isomer would be realized. To conclude, during the synthesis of **1** other isomers could be formed. However, once **1** has been formed it never isomerizes.

Concluding Remarks

The reaction between 1,2-$W_2(^i Bu)_2(O^i Pr)_4$ and H_2 in hydrocarbon solutions has led to the discovery of a novel[27] cluster $W_6(H)_5(C^i Pr)(O^i Pr)_{12}$ (**1**), with an unsymmetrical disposition of ligands such that three hydride ligands "cluster" on one face. The cluster is chemically "inert" and thereby allowed insight into rare site-selective reactions at a cluster. The formation of the hexanuclear cluster, **1**, is proposed to occur by the sequential combination of reactive "W_2" complexes derived from both α- and β-CH activation. This proposal finds support from the trapping of the hydrido alkoxides, **2** and **3**, by the use of chelating phosphines, dmpe and dmpm, respectively.

Experimental Section

General Procedures. All syntheses and sample manipulations were carried out under an atmosphere of dry and deoxygenated nitrogen with standard Schlenk and glovebox techniques. Hydrocarbon solvents were distilled under N_2 from Na/benzophenone and stored over 4 Å molecular sieves. Spectra were recorded on Varian XL-300 (300 MHz), Nicolet NT-360 (360 MHz), and Bruker AM 500 (500 MHz) spectrometers in dry and deoxygenated benzene-d_6, toluene-d_8, or pyridine-d_5. All ^{1}H and ^{13}C NMR chemical shifts are reported in ppm relative to the residual protio impurities or ^{13}C signals of the deuterated solvents. ^{31}P NMR chemical shifts were calibrated against an external sample of H_3PO_4 set at 0.0 ppm. ^{2}H NMR spectra were recorded in benzene or toluene, and the chemical shifts are reported in ppm relative to the natural abundance ^{2}H present in the protio solvent. Infrared spectra were obtained from KBr pellets or Nujol mulls with a Nicolet S10P FT-IR spectrometer. Elemental analyses were performed by Atlantic Microlab, Inc., Norcross, GA, and Oneida Research Services, New York, NY.

Chemicals. The preparation of 1,2-$W_2(^i Bu)_2(O^i Pr)_4$[28] and $W_2(CH_2R)_2(O^i Pr)_4$(dmpm) (R = Ph, ^{i}Bu)[11] was described previously. The ligands dmpe, dmpm, and dppe were purchased commercially and used as received. $W_2(^i Bu)_2(O^i Pr\text{-}d_7)_4$ was prepared from the reaction between 1,2-$W_2(^i Bu)_2(NMe_2)_4$ and $DO^i Pr\text{-}d_7$. All lecture bottles of gases (H_2, D_2, and H_2CCH_2) were rated as 99+% pure and were used as received.

$W_6(H)(\mu\text{-}H)_4(\mu\text{-}C^i Pr)(O^i Pr)_5(\mu\text{-}O^i Pr)_7$ (1). In a 30 mL capacity Kontes solvent seal flask, 1,2-$W_2(^i Bu)_2(O^i Pr)_4$ (0.650 g, 0.905 mmol) was dissolved in *ca*. 15 mL of hexane. The solution was frozen in liquid nitrogen and the flask evacuated and closed. Next, the flask was transferred to a gas addition manifold where it was immersed in liquid nitrogen. At −176 °C, hydrogen (600 Torr, *ca*. 3 atm at 22 °C) was added. The Kontes tap was closed and the contents of the flask warmed to room temperature while stirring continued. After 48 h the excess hydrogen was released and the reaction mixture was transferred to a standard Schlenk flask. The solvent volume was reduced *in vacuo* and the flask cooled to −20 °C for another 24 h. Crystals were isolated by removing the mother liquor and washing with cold hexane (yield: 0.214 g, 38%). Anal. Calcd (found) for $C_{40}H_{96}O_{12}W_6$: C, 25.66 (25.81); H, 5.17 (5.08); N, 0.00 (0.00). ^{1}H NMR (300 MHz, 22 °C, benzene-d_6): W−*H*, δ 14.65 (dd, 1H, $J^{183}{}_{W-^1H} = 88.2$ Hz, 24.5%, $J^1{}_{H-^1H} = 10.6$ Hz, $J^1{}_{H-^1H} = 1.5$ Hz), δ 13.42 (s, 1H, $J^{183}{}_{W-^1H} = 93.4$ Hz, 24.5%), δ 13.40 (s, 1H, $J^{183}{}_{W-^1H} = 105.5$ Hz, 24.5%), δ 10.00 (s, 1H, $J^{183}{}_{W-^1H} = 130.2$ Hz, 14.3%), δ 9.14 (d, 1H, $J^{183}{}_{W-^1H} = 103.5$ Hz, 24.5%, $J^1{}_{H-^1H} = 10.6$ Hz); OC*H*$(CH_3)_2$, δ 5.97, 5.80 (2H), 5.65, 5.56, 5.41, 5.15, 5.10, 4.98, 4.90, 4.85, 4.84 (quintets, 12H, $J^1{}_{H-^1H} = 5.7-6.6$ Hz); C*CH*$(CH_3)_2$, δ 7.10 (quintet, 1H, $J^1{}_{H=^1H} = 6.5$ Hz); OCH(C*H*$_3)_2$, δ 1.15−1.8 (multiple overlapping doublets). ^{13}C{^{1}H} (125 MHz, 22 °C, benzene-d_6): O*C*H$(CH_3)_2$, δ 88.6, 84.4, 84.1, 83.1, 82.5, 79.9, 77.1, 76.6, 76.5, 72.1, 71.4, 69.9; OCH(*C*H$_3)_2$, δ 30.44, 30.40 (2C), 29.61, 28.47, 28.12 (2C), 28.06 (2C), 28.02, 27.97, 26.75, 26.66, 25.89, 25.33, 25.29 (2C), 24.91, 24.84, 24.72, 24.58, 24.51, 23.42, 23.10; CCH$(CH_3)_2$, see below. IR (KBr Pellet): $\nu_{WH} = 1794$ ($\nu_{WD} = 1283$), 1451 w, 1375 m, 1325 m, 1160 m, 1115 s, 978 s, 922 s, 837 s, 581 m, 446 w.

$W_6(D)(\mu\text{-}D)_4(\mu\text{-}C^i Pr)(O^i Pr\text{-}d_7)_5(\mu\text{-}O^i Pr\text{-}d_7)$ (1-d_{89}). **1**-d_{89} was prepared in an identical manner as **1** with 1,2-$W_2(^i Bu)_2(O^i P\text{-}d_7)_4$ and D_2 gas. ^{1}H NMR (300 MHz, 22 °C, benzene-d_6): CC*H*$(CH_3)_2$, δ 7.07 (quin, 1H, $J_{HH} = 6.0$ Hz); CCH(C*H*$_3)_2$, δ 1.72 (d, 3H, $J_{HH} = 6.0$ Hz), δ 1.45 (d, 3H, $J_{HH} = 6.0$ Hz). ^{13}C{^{1}H} (125 MHz, 22 °C, benzene-d_6): CCH$(CH_3)_2$, δ 412.5, δ 52.3, δ 35.7, δ 32.2.

$W_6(D)(\mu\text{-}D)_4(\mu\text{-}C^i Pr)(\mu\text{-}O^i Pr)_7(O^i Pr)_5$ (1-d_5). **1**-d_5 was prepared in the same manner as **2** with D_2 in place of H_2. ^{2}H NMR (22 °C, benzene): δ 14.3 (1D, $J^{183}{}_{W-^2H} = 12.7$ Hz), δ 13.4 (2D, $J^{183}{}_{W-^2H} = 15.7$ Hz), δ 9.88 (1D, $J^{183}{}_{W-^2H} = 20.0$ Hz), δ 8.84 (1D, $J^{183}{}_{W-^2H} = 16.5$ Hz).

$W_2(\mu\text{-}H)_2(dmpe)_2(O^i Pr)_4$ (2). In a 30 mL capacity Kontes brand solvent seal flask, 1,2-$W_2(^i Bu)_2(O^i Pr)_4$, (0.900 g, 1.25 mmol) was dissolved in *ca*. 15 mL of toluene. The chelating diphospine dmpe (0.376 g, 2.51 mmol) was then added from a microliter syringe. The mixture was frozen in liquid nitrogen and the flask evacuated and closed. Next, the flask was transferred to a gas addition manifold where it was immersed in liquid nitrogen. At −176 °C, hydrogen (600 Torr, *ca*. 3 atm at 22 °C) was added. The Kontes tap was closed and the contents of the flask warmed to room temperature while stirring

(26) This is typically catalyzed by alkoxides of Al or Zr, e.g. $Al(O^i Pr)_3$ or $Zr(O^i Pr)_4$: March, J. In *Advanced Organic Chemistry: Reactions, Mechanisms and Structure*, 3rd ed.; J. Wiley and Sons: New York, 1985; pp 811 and 813−814.

(27) The most similar group of octahedral polyhydrido clusters of which we are aware are those recently reported by Cotton and co-workers such as $Zr_6X_{18}H_5{}^{3-}$ and related species, where X = Cl or Br. These have edge-bridging and terminal halides supporting an octahedral Zr_6 unit and the hydrides occupy μ_3-H positions on faces. The hydrides in these anions are fluxional, giving rise to one ^{1}H NMR signal in solution. See: Chen, L.; Cotton, F. A.; Wojtczak, W. A. *Angew. Chem., Int. Ed. Engl.* **1995**, *34*, 1877. $Zr_6(H)_4Cl_{14}(PR_3)_4$: Chen, L.; Cotton, F. A.; Wojtczak, W. A. *Inorg. Chem.* **1996**, *35*, 2988. $Zr_6(H)_5Cl_{18}{}^{2-}$: Chen, L.; Cotton, F. A. *Inorg. Chem.* **1996**, *35*, 7364. Cotton, F. A.; Chen, L.; Schultz, A. J. *C. R. Acad. Sci. Paris* **1996**, *323*, 539.

(28) Chisholm, M. H.; Eichhorn, B. W.; Folting, K.; Huffman, J. C.; Tataz, R. J. *Organometallics* **1986**, *5*, 2171.

(29) Chisholm, M. H.; Folting, K.; Huffman, J. C.; Kirkpatrick, C. C. *Inorg. Chem.* **1984**, *23*, 1021.

continued. After 24 h the excess hydrogen was released and the reaction mixture was transferred to a standard Schlenk flask. The solvent volume was reduced *in vacuo* until crystallization began. The reaction mixture was then warmed gently to regain homogeneity. The flask was left standing at room temperature for several hours and then cooled to −20 °C for another 24 h. Two crops of crystals were isolated in this manner by removing the mother liquor and washing with cold hexane (yield: 0.985 g, 87%). Anal. Calcd (found) for $C_{24}H_{62}O_4P_4W_2$: C, 31.81 (31.94); H, 6.89 (6.95). ^{1}H NMR (300 MHz, +60 °C, toluene-d_8): δ 4.65 (quin, 4H, OC(H)(CH$_3$)$_2$, J_{HH} = 5.7 Hz), δ 1.41 (d, 24H, OC(H)(CH_3)$_2$, J_{HH} = 5.7 Hz), δ 1.62 (bs w/shoulder, 32H, (CH_3)$_2$PCH_2CH_2P(CH_3)$_2$). ^{1}H NMR (300 MHz, −60 °C, toluene-d_8, W−μ-H): δ −12.4 (m, $J_{H-^{31}P}$ = 30.9 Hz), δ −1.60 (m, $J_{H-^{31}P}$ = 15.3 Hz, $J_{H-^{31}P}$ = 6.3 Hz), δ −1.04 (m, $J_{H-^{31}P}$ = 6.3 Hz). ^{2}H NMR (300 MHz, −60 °C, toluene, W−μ-H): δ −12.3 (bs), δ −1.50 (bs), δ −0.90 (bs). ^{31}P{^{1}H} NMR (146 MHz, +60 °C, toluene-d_8), δ 14.9 (bs, dmpe). ^{31}P{^{1}H} NMR (146 MHz, −60 °C, toluene-d_8): δ 18.71 (bs, 2P, ^{183}W−^{31}P = 224.8 Hz), δ 14.37 (s, 1P, ^{183}W−^{31}P = 275.5 Hz), δ 5.91 (bs, 1P, ^{183}W−^{31}P = 167.0 Hz). IR (KBr Pellet): ν_H = 1755 (ν_D = 1250), 1460 w, 1449 w 1420 m, 1366 m, 1348 m, 1331 m, 1316 m, 1290 w, 1277 w, 1265 w, 1161 s, 1117 s, 979 s, 953 s, 885 s, 826 s, 779 w, 716 m, 669 m, 608 s, 594, 446 m, 421 w.

W$_2$(μ-H)$_2$(dppe)$_2$(O^{i}Pr)$_4$. In a 30 mL capacity Kontes brand solvent seal flask, 1,2-W$_2$(^{i}Bu)$_2$(O^{i}Pr)$_4$ (1.00 g, 1.39 mmol) and dppe (1.11 g, 2.78 mmol) were dissolved in *ca*. 15 mL of toluene. The mixture was frozen in liquid nitrogen and the flask evacuated and closed. Next, the flask was transferred to a gas addition manifold where it was immersed in liquid nitrogen. At −176 °C hydrogen (600 Torr, *ca*. 3 atm at 22 °C) was added. The Kontes tap was closed and the contents of the flask warmed to room temperature while stirring continued. After 24 h a large amount of dark precipitate formed. The excess hydrogen was released and the product (1.280 g) collected over a medium porosity frit and washed with hexane multiple times to ensure removal of any dppe. The combined mother liquor and washings were then stripped to dryness *in vacuo*. The solid was then washed several times to remove any hexane-soluble material. A second crop (0.330 g) of the hexane-insoluble product was then collected as before (yield: 1.610 g, 83%). Anal. Calcd (found) for $C_{64}H_{78}O_4P_4W_2$: C, 54.79 (54.94); H, 5.60 (5.61). ^{1}H NMR (300 MHz, 22 °C, benzene-d_6): δ 0.01 (m, 2H, W−H, $J_{^{183}W-^1H}$ = ca. 80 Hz), δ 4.52 (bs, 4H, OCH(CH$_3$)$_2$, δ 1.33 (d, 12H, OCH(CH_3)$_2$), δ 1.03 (bs, 12H, OCH(CH_3)$_2$), δ 2.35, 2.20, 1.68, 0.68 (bm, 8H, Ph$_2$PCH_2CH_2PPh$_2$). ^{31}P{^{1}H} NMR (146 MHz, 22 °C, pyridine-d_5): δ 42.0 (s, 2P, ^{183}W−^{31}P = 291.7 Hz, 14.3%), δ 25.8 (s, 2P, $^1{}_{^{183}W-^{31}P}$ = 161.0 Hz, 14.3%, $^2{}_{^{183}W-^{31}P}$ = 46.0 Hz, 14.3%).

W$_4$(μ-H)$_4$(dmpm)$_3$(O^{i}Pr)$_8$ (3). In a 30 mL capacity Kontes brand solvent seal flask, 1,2-W$_2$(^{i}Bu)$_2$(O^{i}Pr)$_4$(dmpm) (0.400 g, 0.468 mmol) was dissolved in *ca*. 15 mL of hexane. The solution was frozen in liquid nitrogen and the flask evacuated and closed. Next, the flask was transferred to a gas addition manifold where it was immersed in liquid nitrogen. At −176 °C hydrogen (600 Torr, *ca*. 3 atm at 22 °C) was added. The Kontes tap was closed and the contents of the flask warmed to room temperature while stirring continued. After 24 h the excess hydrogen was released and the precipitated product was collected over a medium porosity frit and washed with hexane (yield: 0.163 g, 43%). Anal. Calcd (found) for $C_{39}H_{102}O_8P_6W_4$: C, 28.91 (28.94); H, 6.54 (6.36); N, 0.00 (0.00). ^{31}P{^{1}H} NMR (146 MHz, −60 °C, toluene-d_8): δ −30.94 (m, 1P), δ -21.30 (m, 2P), δ −14.45 (bs, 3P). ^{1}H NMR (300 MHz, +60 °C, toluene-d_8): δ 4.71 (quin, 9H, OC(H)(CH$_3$)$_2$, J_{HH} = 6.0 Hz), δ 1.41 (d, 48H, OC(H)(CH_3)$_2$, J_{HH} = 6.0 Hz), δ 2.20 (bs, 12H, (CH_3)$_2$PCH$_2$P(CH_3)$_2$), δ 1.94 (bs, 12H, (CH_3)$_2$PCH$_2$P(CH_3)$_2$), δ 1.55 (bs, 12H, (CH_3)$_2$PCH$_2$P(CH_3)$_2$). ^{1}H NMR (300 MHz, −60 °C, toluene-d_8): W−H, δ −0.96 (m, 1H), δ-4.15 (d, 1H), δ −7.16 (bs, 1H).

Crystallographic Studies. General operating procedures and listings of programs have been given previously.[29]

W$_6$(H)(μ-H)$_4$(μ-C^{t}Pr)(O^{i}Pr)$_5$(μ-O^{i}Pr)$_7$ (1). A needle shaped crystal was mounted in a nitrogen atmosphere glovebag with silicone grease and it was then transferred to a goniostat where it was cooled to −170 °C for characterization and data collection. A systematic search of a limited hemisphere of reciprocal space revealed no symmetry among the observed intensities. An initial choice of space group $P\bar{1}$ was later proven correct by the successful solution of the structure. Following complete intensity data collection and correction for absorption, data processing gave a residual of 0.036 for the averaging of 1888 unique intensities which had been observed more than once. Four standards measured every 400 data showed no significant trends. The structure was solved by using a combination of direct methods (SHELXS-86) and Fourier techniques. The positions of the tungsten atoms were obtained from an E-map. The remaining non-hydrogen atoms were obtained from subsequent iterations of least-squares refinement and difference Fourier calculation. Hydrogens bonded to carbon were included in fixed calculated positions with thermal parameters fixed at one plus the isotropic thermal parameter of the atom to which they were bonded. The hydride ligands could not be determined by this work. They were included in the formulas and the density calculation since their presence was established by earlier NMR work. In the final cycles of refinement, the non-hydrogen atoms were varied with anisotropic thermal parameters to a final $R(F)$ = 0.048. The largest peak in the final difference map was a tungsten residual of 2.6 e/Å^3. All of the more significant peaks were in chemically unreasonable positions (mostly too close to W) to be interpreted as the anticipated hydride ligands.

Prompted by the fact that spectroscopic results were inconsistent with the original structure and in part by the supporting observation that one of the oxygen atoms, O(15), had an isotropic thermal parameter that was twice as large as for any other oxygen in the structure, data was reevaluated. While a large thermal parameter such as this is not impossible, it probably should have been cause for more concern earlier.

O(15) has now been refined as a carbon, C(15). The isotropic thermal parameter is now at a more reasonable value ($10B_{iso}$ is 15 rather than 50), although the anisotropic thermal parameters for it and two other carbons, C(33) and C(36), did not refine properly. This may be due to absorption errors. The crystal was quite small and the measurements of the crystal dimensions needed for the absorption correction were not accurate and in fact were adjusted somewhat in an attempt to improve the correction.

In the final cycles of refinement. C(15), C(33), and C(36) were varied with isotropic thermal parameters and all other non-hydrogen atoms were varied with anisotropic thermal parameters. Hydrogens bonded to carbon atoms were included in fixed calculated positions. Since changing one oxygen to a carbon is only a change of two electrons in this very heavy atom structure, it is not surprising that the residuals were not significantly different. $R(F)$ was 0.048 as before and the final difference map again had a maximum of 2.6 and a minimum of −2.0 e/Å^3.

W$_2$(μ-H)$_2$(dmpe)$_2$(O^{i}Pr)$_4$ (2). A cube-shaped crystal of suitable size was cleaved from a large piece of the sample in a nitrogen atmosphere glovebag. The crystal was mounted with silicone grease and it was then transferred to a goniostat where it was cooled to −160 °C for characterization and data collection. A systematic search of a limited hemisphere of reciprocal space revealed a primitive monoclinic cell. Following complete intensity data collection the conditions $h + 1 = 2n$ for $h01$ and $k = 2n$ for $0k0$ uniquely determined space group $P2_1/n$. After correction for absorption, data processing gave a residual of 0.054 for the averaging of 887 unique intensities which had been measured more than once. Four standards measured every 400 data showed no significant trends.

The structure was solved by using a combination of direct methods (MULTAN78) and Fourier techniques. The positions of the tungsten atoms were obtained from an initial E-map. The positions of the remaining non-hydrogen atoms were obtained from subsequent iterations of least-squares refinement and difference Fourier calculations. Only a few of the hydrogens were observed. Hydrogens were included in fixed calculated positions with thermal parameters fixed at one plus the isotropic thermal parameter of the atom to which they were bonded.

In the final cycles of refinement, the non-hydrogen atoms were varied with anisotropic thermal parameters to a final $R(F)$ = 0.033. The largest peaks in the final difference map were tungsten residuals of 0.7 to 2.0 e/Å^3. All other peaks were less than 0.6 e/Å^3. The largest hole was −2.1 e/Å^3.

W$_4$(μ-H)$_4$(dmpm)$_3$(O^{i}Pr)$_8$ (3). A crystal of suitable size was mounted in a nitrogen atmosphere glovebag with silicone grease and it was then transferred to a goniostat where it was cooled to −150 °C for characterization and data collection. A systematic search of a

Table 7. Summary of Crystal Data

	I	II	III
empirical formula	$C_{40}H_{96}O_{12}W_6$	$C_{24}H_{60}O_4P_4W_2$	$C_{39}H_{98}O_8P_6W_4$
color of crystal	black	black	black
crystal dimens (mm)	0.08 × 0.10 × 0.36	0.20 × 0.20 × 0.20	0.16 × 0.45 × 0.45
space group	$P\bar{1}$	$P2_1/n$	Pcab
temp (°C)	−170	−160	−150
cell dimens			
a (Å)	12.800(3)	9.841(1)	21.396(3)
b (Å)	20.561(5)	20.478(3)	30.729(5)
c (Å)	11.839(3)	17.280(3)	17.624(2)
α (deg)	103.74(1)		
β (deg)	116.61(1)	95.70	
γ (deg)	88.00(1)		
Z (molecules/cell)	2	4	8
vol (Å)	2696.81	3464.78	11587.86
d_{calad} (g cm^{-3})	2.306	1.734	1.853
wavelength (Å)	0.71069	0.71069	0.71069
mol wt	1872.29	904.33	1616.44
linear abs coef (cm^{-1})	130.719	69.851	82.907
detector to sample dist (cm)	22.5	22.5	22.5
sample to source dist (cm)	23.5	23.5	23.5
av *ω* scan width at $^1/_2$ height	0.25	0.25	0.25
scan speed (deg/min)	6.0	8.0	8.0
scan width (deg + dispersion)	2.0	1.8	1.4
individual background (s)	6	4	4
aperture size (mm)	3.0 × 4.0	3.0 × 4.0	3.0 × 4.0
2*θ* range	6−45	6−45	6−45
total no. of reflcns collected	9059	5669	14614
total no. of unique intensities	7067	4550	7602
total no. with $F > 0.0$	6539	4394	6653
total no. with $F > 3\sigma(F)$	5942	4252	3901
R(*F*)	0.0483	0.0330	0.0372
Rw(*F*)	0.0486	0.0353	0.0381
goodness of fit for last cycle	1.303	1.374	1.227
max δ/σ for last cycle	0.002	0.122	0.051

limited hemisphere of reciprocal space revealed a primitive orthorhombic cell. Following complete intensity data collection, the observed conditions $1 = 2n$ for $0kl$, $h = 2n$ for $h01$, and $k = 2n$ for $hk0$ uniquely determined space group *Pcab*. After correction for absorption, data processing gave a residual of 0.092 for the averaging of 4707 unique intensities which had been observed more than once. The rather large residual is probably due to the fact that there was a large amount of weak data. Of the 7602 unique data, only 3901 were considered observed by the criterion $I > 3\sigma(I)$. Four standards measured every 400 data showed no significant trends. The structure was solved by using a combination of direct methods (MULTAN78) and Fourier techniques. The positions of the tungsten atoms were obtained from an E-map. The remaining non-hydrogen atoms were obtained from subsequent iterations of least-squares refinement and difference Fourier calculation. Hydrogens were included in fixed calculated positions with thermal parameters fixed at one plus the isotropic thermal parameter of the atom to which they were bonded. In the final cycles of refinement, the tungsten atoms were varied with anisotropic thermal parameters and the remaining non-hydrogen atoms were varied with isotropic thermal parameters to a final $R(F) = 0.037$ for 250 parameters varied with the 3901 observed data. The largest peaks in the final difference map were tungsten residuals of 0.78−1.73 e/Å^3. All other peaks were less than 0.77 e/Å^3. The largest hole was −1.14 e/Å^3. The nonbonded W(2)−W(3) distance, not shown in the tables, is 3.618(1) Å.

The program XHYDEX[20] was used to determine optimal hydride positions in compounds **1**, **2**, and **3**. M−H distances were taken to be 1.73 Å for terminal sites and 1.87 Å for bridging sites. The *xyz* coordinates located for hydrides by the program for each molecule are listed in Table 7. In all cases the potential energy values fell between 0 and 2.5 units.

Table 8. The *xyz* Coordinates of **1**, **2**, and **3**

$W_2(H)(\mu\text{-}H)_4(\mu\text{-}C^iPr)$ $(\mu\text{-}O^iPr)_7(O^iPr)_5$ (**1**)			
W(1)−H−W(4)	0.9653	0.1846	0.0465
W(3)−H−W(4)	0.7577	0.2278	−0.0328
W(3)−H−W(5)	0.5859	0.1971	−0.2230
W(4)−H−W(5)	0.7781	0.1251	−0.1452
W(6)−H	0.9739	0.4098	0.0866
$W_2(\mu\text{-}H)_2(dmpe)_2(O^iPr)_4$ (**2**)			
W(1)−H−W(2)	0.2220	0.1717	0.6957
W(1)−H−W(2)	0.4832	0.1457	0.7674
$W_4(\mu\text{-}H)_4(dmpm)_3(O^iPr)_8$ (**3**)			
W(1)−H−W(2)	0.0971	0.1011	0.0791
W(2)−H−W(3)	0.1195	0.2172	0.1268
W(3)−H−W(4)	0.1254	0.2979	0.1865
W(3)−H−W(4)	0.1438	0.3261	0.0436

Acknowledgment. We thank the Department of Energy, Office of Basic Sciences, Chemistry Division for financial support and the reviewers for their careful reading of this manuscript and constructive comments concerning its shortening. Dedicated to Professor Dr. G. Huttner on the occasion of his 60th birthday. For part 1 in this series see ref 8.

Supporting Information Available: Crystallographic data for compounds **1**, **2** and **3** (20 pages). See any current masthead page for ordering and Internet access instructions.

JA9643634